Final Publishable Report

1.1 Please provide an executive summary.

The project "Health Impact of Engineered Metal and Metal Oxide Nanoparticles: Response, Bioimaging and Distribution at Cellular and Body Level", HINAMOX started in October 2009, coordinated by the Centro de Investigación Cooperativa en Biomateriales/CIC BiomaGUNE (Spain), with the following partners: University of Vigo/UVIGO (Spain), University of Leipzig /ULEI (Germany), Research Centre For Applied Chemistry/CIQA (Mexico), Zhejiang University/ZJU (China), PlasmaChem (Germany), National Research Centre For The Working Environment/NRCWE (Denmark), Finnish Institute Of Occupational Health /FIOH(Finland).

Metal oxide nanoparticles (NPs) Al_2O_3, Y_2O_3, TiO_2, ZnO, CeO_{2-x} and Fe_3O_4. NPs were synthesised and characterised regarding, shape, size, size distribution and crystalline structure. potential, stability and aggregation in relevant physiological conditions have been studied as well. NPs have been radiolabelled for biodistribution studies incorporating ^{18}F or ^{13}N.

The uptake, localisation of NPs and their intracellular fate were studied by applying Confocal Raman Microscopy, Transmission Electron Microscopy, Ion Beam Microscopy (IBM) and Confocal Laser Scanning Microscopy. IBM techniques, Proton Induced X ray Emission and Rutherford Backscattering, were used to quantify intracellular amount of NPs and to prove NP internalisation.

Cell viability studies in A549, and ATII primary cells and in other cell lines show a toxicological effect of ZnO NPs while cell viability studies in the same cell lines of other NPs show a non toxic effect. Apoptosis, ROS generation, cytokine activation, and cell path ways were also studied. For ATII cells, NP uptake and the immune response were studied simulating different breathing conditions: static, quiet, and heavy.

Biodistribution studies with Positron Emission Tomography were performed with animal models using radiolabelled NPs following oral, topical, intravenous, and inhalation exposure. NP distribution, accumulation and excretion were monitored over time. The relative activity per organ was measured as an indication of the NP concentration.

The impact of metal oxide NPs on the lung function was evaluated studying the impact of the NPs on the lung function after inhalation, degree of inflammation and genotoxicity. IBM was applied to quantify the amount of NPs in the lung cells after exposure.

Dustiness of NPs and risks on NP preparation/handling in the working place were evaluated. A final risk assessment of the toxicological impact of the NPs was provided.

1.2 Please provide a summary description of the project context and the main objectives.

The project "Health Impact of Engineered Metal and Metal Oxide Nanoparticles: Response, Bioimaging and Distribution at Cellular and Body Level", HINAMOX, started in October 2009, lasting 3 years. HINAMOX was coordinated by the Centro de Investigación Cooperativa en Biomateriales – CIC BiomaGUNE (Spain), with the following partners: University of Vigo/UVIGO (Spain), University of Leipzig/ULEI (Germany), The Research Centre For Applied Chemistry/CIQA (Mexico), Zehjiang University (China)/ZJU, PlasmaChem AG (Germany), The National Research Centre For The Working Environment/NRCWE (Denmark), and The Finnish Institute of Occupational Health (FIOH) (Finland).

Among the large variety of industrially and medically important engineered nanomaterials and nanoparticles (NPs), the HINAMOX project focused on metal and metal oxide NPs as potentially hazardous to biological organisms. Metal oxide and metal NPs are widely used in various industrial processes and commonly used products such as sun creams, surface coatings, electronic devices, fuels, etc.

At least one example of each of the metal oxide NPs with the most relevant applications or potential, according to the Nanomaterial Roadmap 2015 of the 6th Framework programme, were considered for study. Initially the consortium started working with the following NPs: Cerium oxide CeO_{2-x}, titanium oxide TiO_4, zinc oxide ZnO, aluminium oxide Al_2O_3, yttrium oxide Y_2O_4, iron oxide Fe_2O_3, with a focus on the first four oxides.

Metal oxide and metal NPs may be dangerous for humans for two reasons: their special catalytic activity coming from the properties of their nano interface, which may interfere with numerous intracellular biochemical processes, and because of the eventual decomposition of the NPs with the subsequent ion leakage that would increase intracellular ion concentration and could therefore heavily interfere with the intracellular free metal ion homeostasis, which is essential for cell metabolism.

Previous research and hypotheses suggest that the particle size, shape, chemical composition and chemistry of the capping agents determine the catalytic properties and surface activity of NPs as well as of complex materials within which the NPs may have been incorporated. These properties are important regarding the technical application of the NPs and must be studied in the context of their effects on human health. The health impact of the metal oxides NPs must be related to their chemistry and physical properties in order to develop predictive tools for risk evaluation. The substantiated evaluation of the health risk, associated with the exposure to metal oxide and metal NPs, requires therefore a concerted action. The HINAMOX approach was based on a close collaboration within a highly interdisciplinary consortium with expertise in Synthetic Chemistry, NP Production Technology, Material Science, Radiochemistry, Particle Physics and Characterisation, Biochemistry, Toxicology, Immunology, Medicine, " in vivo " Imaging, and Occupational Hygiene.

A very specific problem in dealing with the toxicological evaluation of nanomaterials and in particular with metal oxide NPs is the difficulty of localising and quantifying them in cells and organs. Obtaining dose effect relationships for these NPs is a rather complex task, because of the unknown quantity of material present in affected cells and organs. The actual dose of NPs present in cells and organs for a defined route of exposure and a certain exposed dose will depend on the interaction of the NPs with biological matter, such as proteins in biological fluids, the cell membrane, cell receptors, etc. This interaction depends in turn on the chemistry and physico chemical properties of the NPs, such as size, NP stability, surface chemistry, etc. Obtaining relationships between exposure dose of NPs and the "real" dose that is present in the cells, organs or organism is a rather complex task associated with the physical chemistry of the NPs, their mechanism of interaction with biological matter and the biological fate of the NPs. It is however, fundamental for understanding the impact of NPs on human health. The "real" assimilated dose will bring fundamental knowledge on the immunological action of the NPs. It will also allow the comparison of different exposure scenarios and how these impact on biological functions and immune response. Moreover, the real dose quantification will allow a comparison between "in vitro" and "in vivo" results and will be fundamental in order to validate "in vitro" tests for the toxicological evaluation of NPs and in the definition of regulations related to nano..

The amount of NPs assimilated, both by cells and organs, will depend on multiple factors related to the properties of the NPs. The interaction of the NPs with biomolecules in cell media, with blood components or with lung surfactant, to give some examples, will impact on the physical state and degree of aggregation and on the surface characteristics of the NPs that the cells experience. In cell media, for example, in "in vitro" experiments NPs are surrounded by a layer of proteins, the so called "protein corona". The formation and stability of this corona will determine the interaction of the NPs with cells, with the cell not being in direct contact with the surface of the NPs unless the corona is removed. Also, in the cases where NPs are inhaled, upon reaching the lungs they will interact with the lung surfactants. The lung surfactant will deposit on the surface of the NPs and like the protein corona, define the surface chemistry of the NPs when interacting with lung cells. The association with biomolecules can lead to aggregation of NPs, resulting in structures with sizes even in the micro range. The state of aggregation and the chemistry of the NPs will have an influence on their uptake mechanism and the amount of NPs assimilated. Also, when the NPs have translocated inside the cells, the state of aggregation and the nature of the surface chemistry of the NPs or the biomolecules associated with the NPs will determine their interaction with the cell machinery. The intracellular localisation is also fundamental in understanding the biological action of the NPs. In the same way, it is fundamental to determine which organs are affected by the NPs when they penetrate an organism by the different exposure pathways and how NPs behave over time while in an organism, when they are excreted or if they accumulate, if the affected organs present inflammation. The HINAMOX consortium have applied a battery of experimental techniques to determine the cellular fate of NPs and their real intracellular concentration: Transmission Electron Microscopy, Ion Beam Microscopy: Rutherford Backscattering Spectroscopy, Proton Induced X Ray Spectroscopy, Confocal Raman Microscopy, Fluorescence Correlation Spectroscopy, Confocal Laser Scanning Microscopy, Flowcytometry, and Inductively Coupled Plasma Mass Spectrometry. Each technique provides

complementary information leading to a better understanding of NP translocation and fate at the cellular level. Biodistribution studies and NP quantification "in vivo" were performed in animal models (rats) employing Positron Emission Tomography and radiolabelled NPs. The use of radiolabelled NPs allows for the quantification of the relative dose per organ for a given amount of NPs on the basis of the activity per organ, which comes from the radiolabelled NPs present.

The biological fate of metal oxide NPs and NP quantification at cellular and body level were the focus of the HINAMOX project. In addition, the immune response was also studied "in vitro" employing immortalised and "primary" cell cultures with a focus on the lung function. The immune response was studied with the goal of relating the physical properties of the NPs and the real dose with their toxicological end points. Cell viability, apoptosis, necrosis, complement activation, cytokine activation, cell migration and the generation of reactive oxygen species were studied. The lung function was given priority as the most likely route of exposure to NPs. Also, the impact of the NPs in cell functions and the amount of NPs uptaken were studied in primary cell cultures under different simulated breathing conditions. Also, the immune response was studied for cell lines corresponding to organs affected by the NPs as identified in biodistribution studies. The toxicological impact, on lung function, due to the metal oxide NPs was also studied with animal models. Alterations in respiratory parameters of spontaneously breathing mice were studied as well as inflammation in the lungs after NP inhalation by assessing cell composition and quantifying the number of NPs in the broncho alveolar lavage fluid as well as the genotoxic response. In additon, "dustiness" of the metal oxides NPs under investigation was evaluated as well as the risk of exposure at the NP provider's facilities, PlasmaChem, during NP synthesis, handling and storage. Finally a risk assessment of the NPs was elaborated.

The company PlasmaChem, which is a member of our consortium, provided the consortium with metal oxide NPs. CeO_2 and ZnO NPs were purchased from Evonik, Germany as well. The consortium synthesised NPs with specific fluorescence and radio labels for their biodistribution studies and quantification "in vitro" and " in vivo" respectively.

Characterisation of the structural properties of the commercial NPs and those fabricated by the consortium was a key aspect in this project. Surface and structural properties of NPs were related to their toxicological impact and a strong effort was made in understanding and relating these to the characteristics of the materials, the differences in toxicity, uptake and/or distribution among the NPs under studies. NPs were carefully characterised after labelling to quantify the impact of the labelling on their properties and ensure that are still representative of the original NPs under study.

1.3 Please provide a description of the main S & T results/foregrounds.

The scientific and technological development of HINAMOX can be divided in six major research focuses and will be presented tackling the following issues:

The synthesis and characterization of metal oxide NPs

The quantification and biological fate of the metal oxide NPs at cellular level

Studies of the immune response in vitro

Biodistribution, Biological Fate and Quantification of NPs in vivo

Impact of NP Inhalation on Lung Function

Dustiness and NP Concentration during Production and Handling of Metal Oxide NPs

1) Synthesis and Characterisation of Metal Oxide NPs

Metal oxide NPs were provided by PlasmaChem following their own production protocols. For the work carried out in HINAMOX, with the goal of obtaining NPs with optimised features regarding size, polydispersity, crystallinity, etc., the synthesis protocols of the company were reviewed and improved with the support of CIQA.

A systematic characterisation of the NPs included structural and size characterisation by means of Transmission Electron Microscopy (TEM), size characterisation by means of Dynamic Light Scattering (DLS), surface chemistry by X-ray Photoelectron Spectroscopy (XPS). The photocatalytic activity of the NPs was measured as an estimate of the possible catalytic activity of the NPs in cells.

In addition to the structural properties of the NPs, studies were also performed to investigate their behaviour in biological fluids or in the presence of biologically relevant molecules, looking at aggregation by means of DLS, the evolution of the surface charge by potential measurements, if the surface chemistry of the NPs has been altered by means of XPS and Ion Beam Microscopy, and the stability of the NPs in cell media by means of Atomic Adsorption Spectroscopy.

1.1) Synthesis and Structural Characterisation of unlabelled Metal Oxides NPs

We will describe examples of the work performed in the synthesis and structural characterisation of two of the metal oxide NPs in the project.

1.1.1) Zinc Oxide NPs

Due to a relatively high solubility of ZnO in water (ca. 1.5 mg/l) and a low yield of material in non-aquatic gel-sol processes, precursor pyrolysis was chosen as a preferential synthesis method. A precursor, basic zinc carbonate ($Zn_5(CO_3)_2(OH)_6$), was first prepared by a precipitation reaction from a hot (80 °C) aqueous solution composed of 1 M zinc chloride and sodium carbonate. Nanocrystalline ZnO particles were then obtained by aging the precursor at 375 °C for 0.5 - 20 h. It was found that after 10 min in an oven at 375 °C, a 1 kg batch sample reached a temperature of ca. 270 °C which exceeds the decomposition temperature of basic zinc carbonate (approximately 250°C).

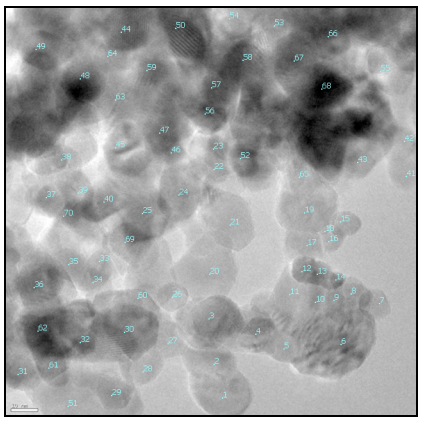

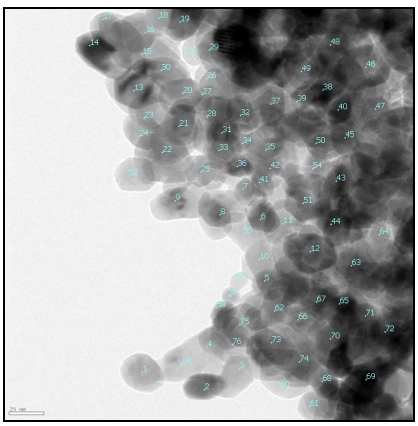

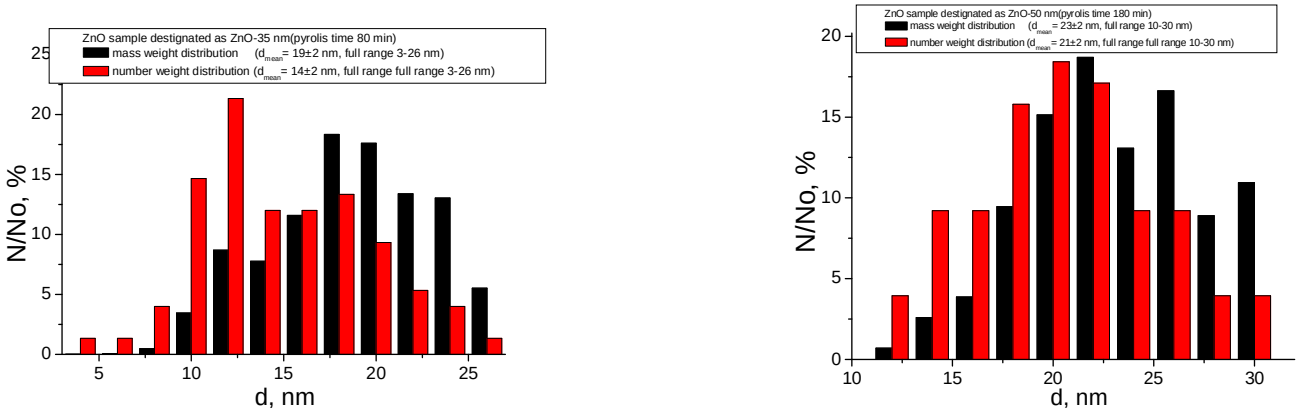

Fig. 1 TEM images (top) and mass and number weight of the particle size distribution evaluated from TEM images (bottom) of ZnO powders prepared by thermolysis of $Zn_5(CO_3)_2(OH)_6$ at 375^0C during 80 min (left) and 300 min (right).

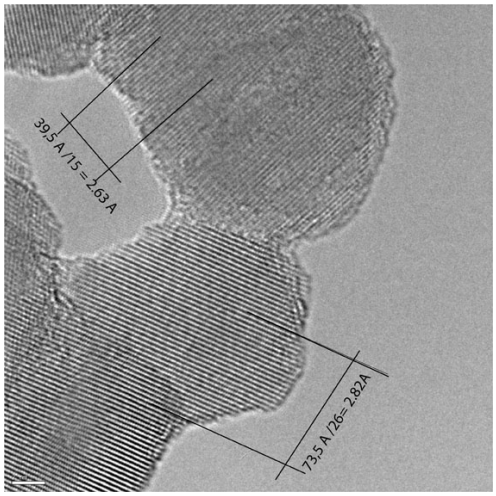

Fig.2 High Resolution Electron Microscopy Image (HREM) of ZnO particles.

Sample morphology and the number and mass weight of the particle size distribution were calculated on the basis of 100 particles, for particles obtained by pyrolysis after 80 minutes and 300 minutes. Particle size increases with increasing calcination time, and range in size from 3 - 26 nm and 10 - 30 nm for the corresponding samples. Most probably, ZnO nanopowders consist of particles consolidated into a porous, reticulated network. HREM provides an estimate of the planar distance of between 2.82 Å and 2.63 Å, which are close to the planar distance for hkl 100 (2.814 Å) and 002 (2.603 Å) and can be indexed as the wurtzite structure of ZnO (classified as JCPDS 36-1451). The wurtzite structure was confirmed by Raman microscopy.

1.1.2) Synthesis of TiO_2 NPs

Colloidal solutions of nanosized titania were prepared at room temperature by 1) hydrolysis of titanium tetrachloride solution with a further condensation of the reaction products, and stabilisation by nitric acid, or 2) by hydrolysis of titanium tetraisopropoxide. A sol gel, prepared from titanium tetrachloride, consists of titania particles in an anatase form as deduced from the Raman Spectra with sizes in the range 5 - 25 nm and a mean particle diameter of 8 nm.

To prepare titania by the hydrothermal method, $TiCl_4$ was used as a starting material and HNO_3 and HCl as stabilising agents. The hydrothermal process in the presence of HNO_3 leads to the formation of particles with the anatase phase.

Raman spectra of dried particles produced using HNO_3 as a stabiliser have features typical of anatase, but with broader bandwidths. Several weaker bands are attributed to the brookite phase. Wide angle X-ray scattering

(WAXS) analysis shows similar results - the major phase is anatase with traces of brookite. The average diameter of TiO_2 NPs as measured by DLS and by small angle X-ray scattering (SAXS) is 16 nm with a full range from 4 nm to 20 nm.

Rutile NPs were prepared via the hydrothermal method with amorphous titania in the presence of HCl.

1.2) Synthesis and Characterisation of Labelled Metal Oxide NPs

The consortium worked on the design of NPs either fluorescently or radio labelled. This was a major issue as the labelling allows tracking the fate of the NPs both *in vitro* and *in vivo*. NPs were carefully characterised after labelling in order to assess the impact of the labelling on their properties and if they are still representative of the original NPs. Two approaches were followed for radiolabelling.

1.2.1) Synthesis of ^{13}N-Radiolabeled NPs

The first attempt to label NPs consisted of the direct irradiation of metal oxide NPs with protons to produce ^{13}N-labelled NPs via the $^{16}O(p, \alpha)^{13}N$ nuclear reaction (Fig. 3). Despite the short half life of ^{13}N (9.97 min) and the relatively high positron energy (Max. Energy = 1.19 MeV), the strategy allowed the production of high amounts of radioactivity with short irradiation times. The methodology developed, which can be applied to any commercially available metal oxide NP irrespective of the metallic atom, is perfectly suited for a fast preliminary screening of the biodistribution pattern of metal oxide NPs depending on, e.g.; particle size, chemical composition, surface charge or crystal phase. Although the residency time of NPs in the body might by far longer than the (radio) activation time, due to the short half life of ^{13}N, valuable information concerning the biodistribution pattern during the first minutes after administration were easily obtained. This strategy was only applied to the production of labelled Al_2O_3 NPs.

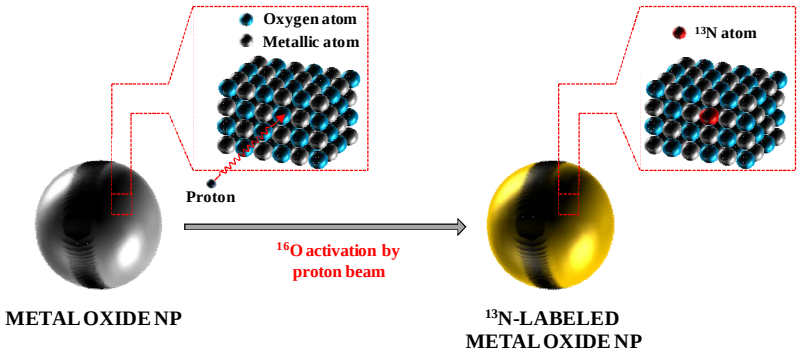

Fig. 3 Activation of aluminum oxide NPs by proton irradiation via the $^{16}O(p,\alpha)^{13}N$ nuclear reaction.

Four different Al_2O_3 NPs with nominal sizes of 10 nm (NS_{10nm}), 40 nm (NS_{40nm}), 150 nm (NS_{150nm}) and 10000 nm ($NS_{10\mu m}$), were exposed to 16 MeV proton irradiation (target current = 5 µA, integrated current = 0.5 µAh). Considering the relative abundance of the radioisotope ($^{13}N/^{18}O$), the amounts of radioactivity obtained at the end of the irradiation process of NS_{10nm}, NS_{40nm}, NS_{150nm} and $NS_{10\mu m}$ NPs were estimated to be >25 MBq/mg in all cases.

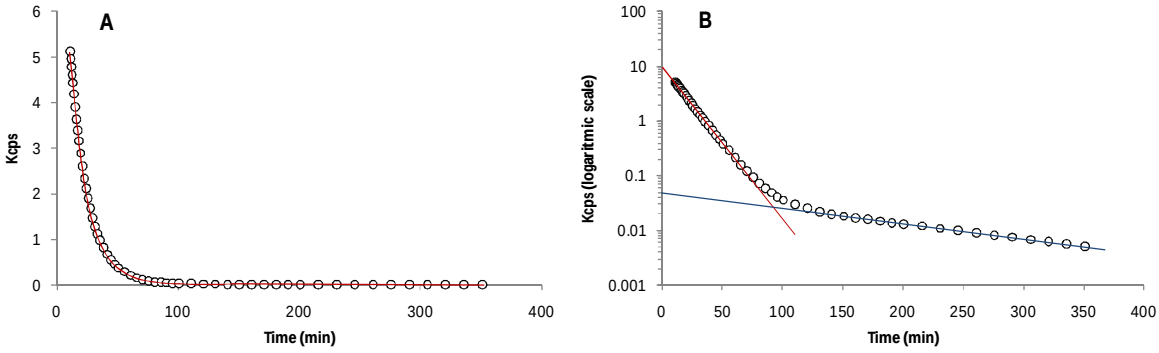

Fig. 4 (A) Decay curve of irradiated Al_2O_3 NPs measured with PET (example of NS_{40nm}); red line corresponds to bi-exponential curve fitting; white dots are experimental measurements. (B) Decay curve with the y axis in logarithmic scale. The two linear regions correspond to ^{13}N (red line) and ^{18}F (blue line). Intersection of the blue line with y axis corresponds to the amount of ^{18}F at the end of the irradiation process. Intersection of the red line with y axis corresponds to the amount of $^{18}F+^{13}N$ at the end of the irradiation process. The slopes of the red and blue lines are inversely proportional to half lives of ^{13}N and ^{18}F, respectively.

The stability of the Al_2O_3 NPs to 16 MeV proton irradiation was determined by TEM and DLS measurements before and after irradiation. Average NP size was determined by TEM before and after irradiation for all NPs (Table 1). Slightly larger values were obtained for DLS measurements for all NPs (Table 1). However, also in this case measurements performed before and after irradiation offered equivalent results within the experimental error. Values of potential (Table 1) were also very similar before and after irradiation. Altogether, these results confirm the stability of alumina particles in aqueous media and indicate no significant modification of the surface charge caused by the irradiation process.

	P.S. (TEM)		**P.S. (DLS)**		**ξ-potential**	
Nanoparticle	**B. I.**	**A. I.**	**B. I.**	**A. I.**	**B. I.**	**A. I.**
NS_{40nm}	35 ± 20	31 ± 19	35.1 ± 8.2	33.1 ± 8.1	20.9 ± 1.3	18.0 ± 3.3
NS_{150nm}	187 ± 92	178 ± 68	266.0 ± 19.5	271.3 ± 18.9	8.6 ± 2.2	10.6 ± 2.8
$NS_{10\mu m}$	-----	-----	2528 ± 225	2824 ± 342	-2.1 ± 2.8	-5.8 ± 1.6

Table 1. Particle size (P.S.) measured by TEM and DLS and ξ-potential values before (B.I.) and after (A.I.) beam for NS_{40nm}, NS_{150nm} and $NS_{10\mu m}$ NPs.

1.2.2) Synthesis of ^{18}F-Radiolabeled NPs

The second strategy to label NPs consisted of the direct irradiation of ^{18}O-enriched metal oxide NPs with protons via the $^{18}O(p, n)^{18}F$ nuclear reaction (Fig. 5). Activation of the NPs using this nuclear reaction yielded NPs containing the commonly used positron emitter ^{18}F (109.8 min half-life, maximum positron energy = 0.69 MeV) in their structure.

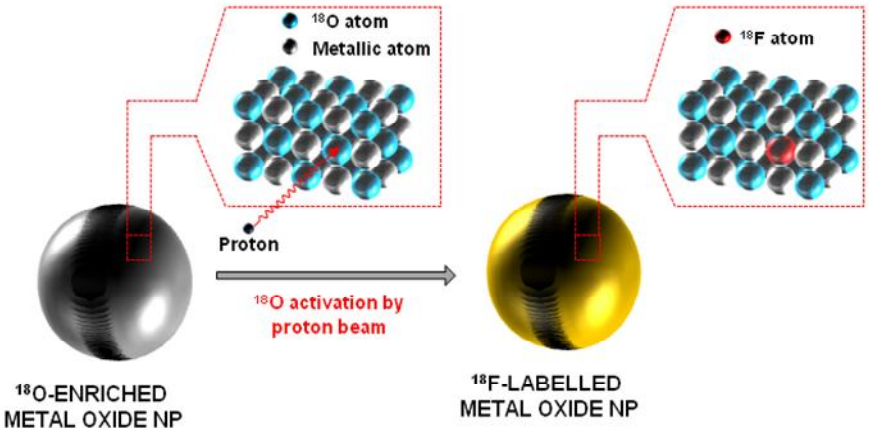

Fig. 5 Activation of ^{18}O-enriched aluminum oxide NPs by proton irradiation via the $^{18}O(p,n)^{18}F$ nuclear reaction.

This methodology allows only activation of ^{18}O-enriched metal oxide NPs, which are not commercially available and were thus prepared in our lab. ^{18}O-enriched metal oxide NPs were prepared by precipitation under basic conditions starting from acidic aqueous solutions of the corresponding metal (Al, Zn and Ti) chloride using ^{18}O-

enriched water as a solvent. NH_3(g) was bubbled into the aluminum salt solution held at room temperature until the precipitate was formed. The resulting precipitate was centrifuged, washed and dried before irradiation.

^{18}O-enriched ZnO, TiO_2 and Al_2O_3 NPs were exposed to 16 MeV proton irradiation (target current = 5 µA, integrated current = 0.5 µAh).

For Al_2O_3 NPs, the relative amount of ^{18}F could be maximised up to >70%, while 30% of ^{13}N was also formed. However, ^{13}N could be eliminated easily just by waiting for it to decay, without significant loss of ^{18}F. In the case of ZnO, ^{68}Ga and ^{66}Ga could also be detected in relative amounts of 30% and 1%, respectively. This was not a drawback for further *in vivo* applications. For TiO_2 NPs, the minor presence of ^{48}V could also be detected. The stability of the ^{18}O-enriched ZnO, TiO_2 and Al_2O_3 NPs to 16 MeV proton irradiation was determined by TEM and DLS before and after irradiation. NP size was determined by TEM (See Fig. 6 for example, Al_2O_3). Slightly larger values were obtained for DLS. Measurements performed before and after irradiation offered equivalent results within the experimental error (Fig. 6 for Al_2O_3). The crystal phase as determined by X-ray diffraction also showed that there was no difference before and after irradiation. Altogether, these results confirm the stability of ^{18}O-enriched ZnO, TiO_2 and Al_2O_3 particles in aqueous media and indicate no significant modification of the structure by the irradiation process.

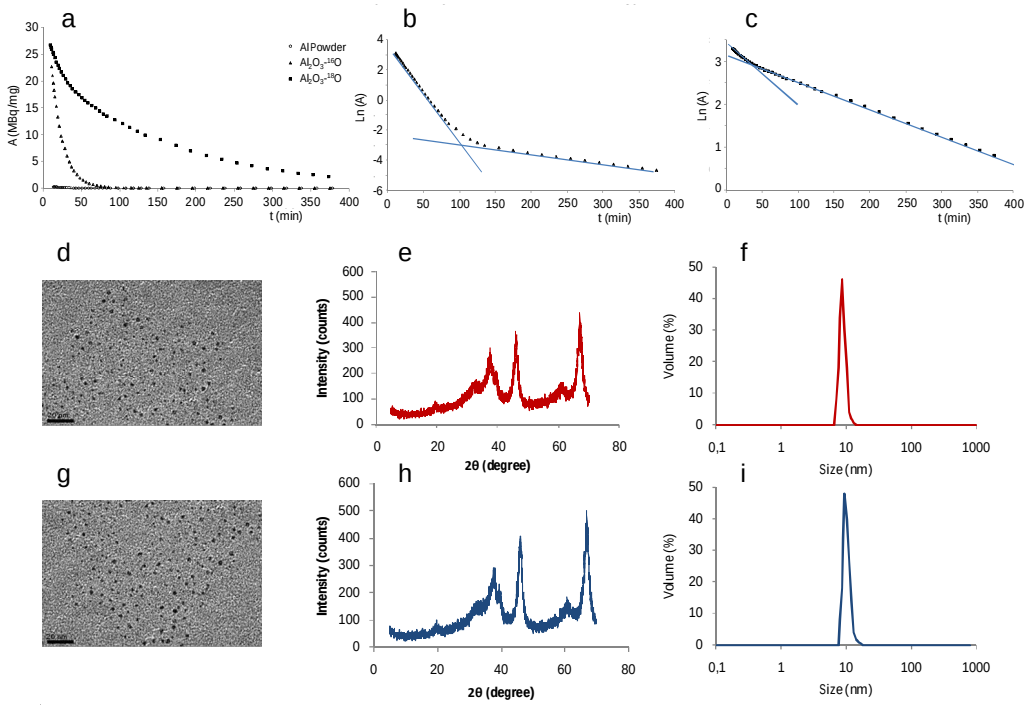

Fig. 6 Transmission Electron Microscopy (TEM) images (**d**, **g**), X-Ray diffractograms (**e**, **h**) and size distribution determined by Dynamic Light Scattering (DLS) (**f**, **i**) for Al_2O_3 NPs synthesised with [^{18}O]H_2O before (**d**, **e**, **f**) and after (**g**, **h**, **i**) irradiation; decay curves obtained for aluminum powder (open circles), NPs synthesised with [^{16}O]H_2O (filled triangles) and NPs synthesised with [^{18}O]H_2O (filled squares) after irradiation (**a**). For [^{16}O]H_2O NPs, two linear ranges can be observed when the Y axis is shown in logarithmic scale, corresponding to the presence of ^{13}N and ^{18}F (**b**). For [^{18}O]H_2O NPs, the linear range for ^{13}N is much shorter because ^{18}F is primarily produced during irradiation (**c**).

1.3) Characterisation of NPs in Biologically Relevant Environments

DLS experiments were performed to provide an additional verification of the size of NPs, evaluate sample polydispersity and to follow NP aggregation in different aqueous environments. DLS allows the comparison of NPs in solutions of different ionic strength and composition and to determine to what extent the characteristics of the media may induce aggregation. DLS experiments were performed in milliQ water, physiological solution, PBS solution, in Serum and in DMEM, DME Glutamax, and RPMI, the different cell media used in the project.

The degree of aggregation in aqueous media varied from NP to NP but all the NPs showed limited polydispersity. Increasing ionic strength, the presence of PBS and proteins and the suspension in cell media all cause aggregation. Suspension in cell media causes the highest degree of aggregation resulting in aggregates of several, even hundreds of, microns in diameter.

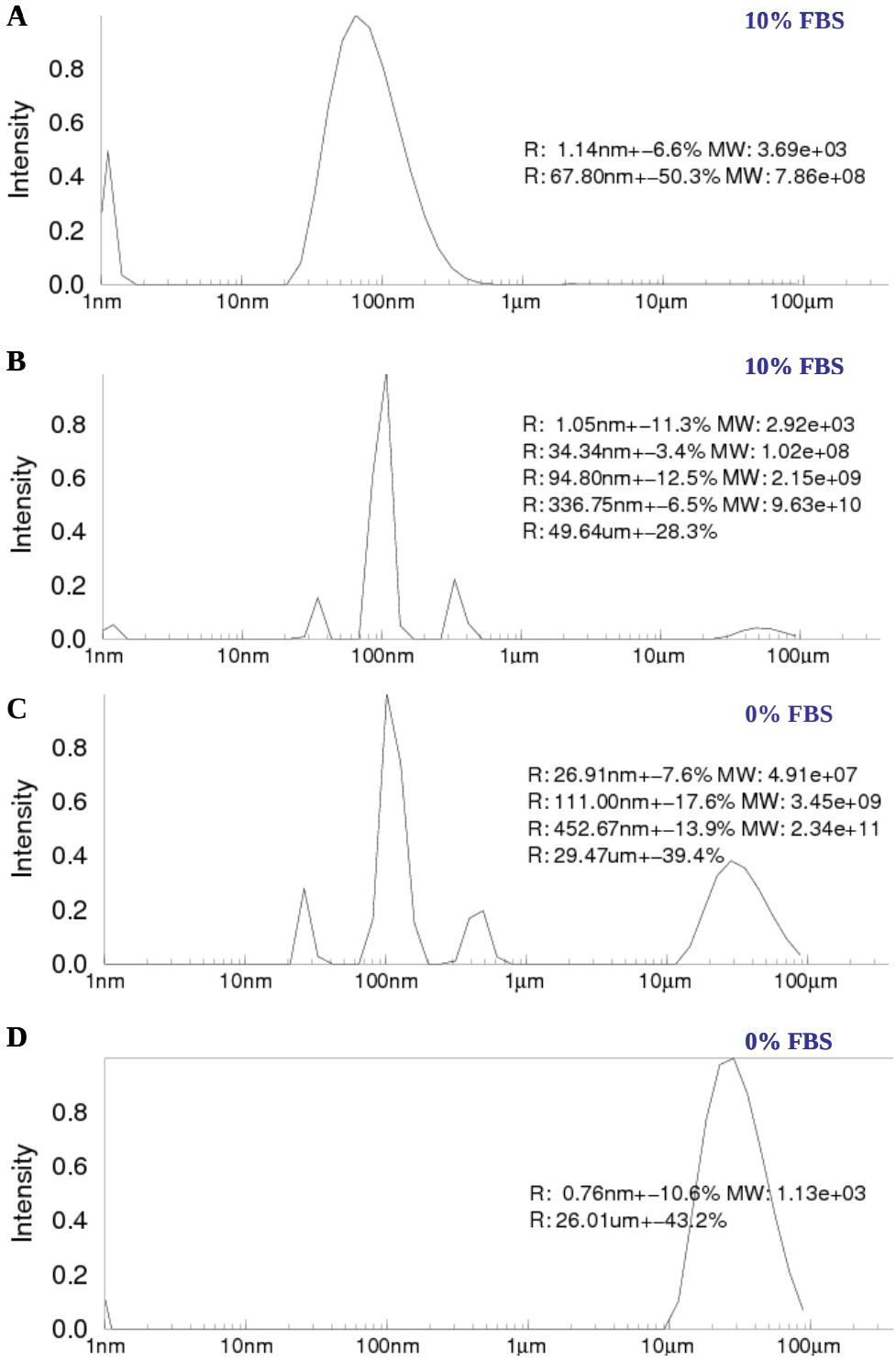

Fig. 7 DLS of ZnO NPs treated by means of tip sonication (A, C) and water bath sonication.

DLS was used to determine the optimal conditions for stabilising the NPs in cell media while avoiding/minimising aggregation. A protocol was developed to improve dispersion of NPs, using fetal calf serum (FBS) during NP

fabrication via sonication. Figure 7 A, B, C, D compares the DLS measurements and degree of aggregation of ZnO NPs under different sonication conditions and different percentages of FBS in solution.

ζ-potential measurements were performed in solutions of different ionic strength and pH, in PBS, fetal bovine serum, physiological media, DMEM, DMEM + Glutamax, and RPMI. All NPs have a positive potential in NaCl regardless of salt concentration with the exception of the TiO_2 NPs from Degussa which have a negative potential.

In PBS all the NPs acquire a negative value between -18 and -22 mV. The reversing of the potential and the fact that all the NPs display a similar ζ potential is indicative of the adsorption of the phosphate molecules. The phosphate buffer solution contains diphosphate salts. These bear two charges and can therefore form a complex with the NPs, if they are positively charged, and reverse the charge of the NPs to negative values simultaneously. The complexation of phosphate molecules and the change in potential of the NPs is an important issue since it implies a change in the surface properties of the NPs and therefore in their interaction with cells and biomolecules.

In the different culture media NPs show almost identical potential values: around -10 mV in DMEM; between -5 and -10 mV in DMEM + Glutamax, with the exception of CeO_2 NPs with approximately a 0 potential in this media. These values are not very different from NPs in PBS.

XPS experiments were performed on NPs exposed to PBS or cell media and carefully washed afterwards. These experiments were done to assess if the phosphate salts or (eventually) proteins attach to the NP surface. XPS allowed the presence of phosphorus to be identified at the surface of the CeO_2 and ZnO NPs but not at the surface of the Al_2O_3 or TiO_2 NPs. This is the case for both the treatment with PBS solution and the DMEM media. The presence of phosphorus is indicative of selective complexation of the phosphate molecules to the NPs since no phosphorus could be detected for the NPs before treatment with PBS.

The composition of NPs was also studied by means of Ion Beam Microscopy (IBM). Elemental mapping both in culture medium show elemental mappings of ZnO and CeO_2 NP clusters in cell culture medium (RPMI). The data show that Ca and P are always found together with ZnO and CeO_2 NPs. This is more clearly demonstrated in the concentration profiles recorded in the selected region. Here the co-localisation of P and Ca with ZnO NPs and the co-localisation of Ca with CeO_2 NPs is demonstrated. On the contrary, no co-localisation with Ca and P was found in the case of TiO_2 and FeO_x NPs.

Solubility of NPs in cell culture media was measured by Atomic Absorption Spectrometry (AAS). It was found that ZnO particles could significantly dissolve and reached quite a high Zn^{+2} ion concentration (~1 µg/ml) within 4 hours, Fe_3O_4 NPs showed lower solubility (~0.01 µg/ml), while TiO_2 NPs showed very poor solubility (<0.00001 µg/ml).

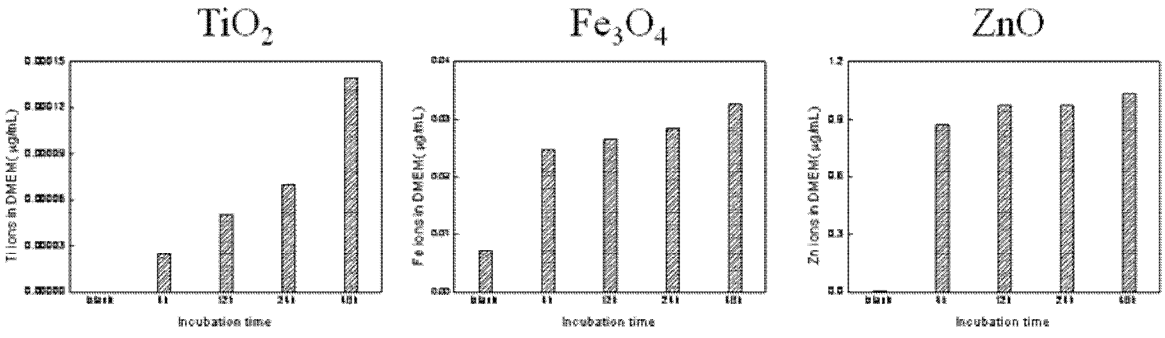

Fig. 8 Free element concentration detected by AAS as a function of the incubation time in DMEM/10% FBS.

2) Quantification and Biological Fate of Metal Oxide NPs at the Cellular Level

The uptake and processing of metal oxide NPs by cells will depend on the characteristics of the NPs, their surface chemistry and their interaction with proteins and other biologically relevant molecules, and the administration method.

The process of uptake will determine the real amount of NPs present in the cell, the so called Genuine Dose. The Genuine Dose is the critical link between exposure and toxicity and can be considered as a key toxicological

endpoint. Therefore the quantification of the Genuine Dose is a basis for systematic and comparable intracellular dose dependent toxicity studies between *in vitro* and *in vivo* tests.

The Ion Beam Microscopy technique (IBM) has been employed in HINAMOX as a means of determining the amount of metal oxide NPs present in the cells down to subcellular resolution and as proof of their internalisation. The amount of NPs internalised was studied as a function of the exposure dose and surface modification of NPs. A protocol was developed within the consortium to stabilise the NPs with FBS in order to improve dispersion and avoid/minimise aggregation. However, this stabilisation has an effect upon NP uptake.

The intracellular concentration of Zn^{+2} ions was also determined by fluorescence techniques resulting from the degradation of ZnO NPs.

TEM, Confocal Laser Scanning Microscopy (CLSM), and Confocal Raman Microscopy (CRM) were combined with IBM to gain a better understanding of the processing of NPs by the cell, their location and translocation with time.

Also the interaction of the NPs with proteins was studied regarding their impact on uptake.

2.1) Quantification of NP Uptake and Determination of Toxicologically Relevant Doses by means of IBM

Proton Induced X Ray Emission (PIXE) and Rutherford Back Scattering (RBS) were applied simultaneously to A549 cells, previously exposed to NPs. The NP distribution and their intracellular concentration were determined. Fig. 9 shows PIXE images of cells exposed to different metal oxide NPs. All surface modified NPs were applied at a concentration of 30 µg/ml for 48 h. The top row of images represent the sulphur elemental distribution of treated cells. Sulphur as well as phosphor are the main elements in cells and were used for the purpose of visualising single cells. The bottom row of images displays the representative NP distributions within or on top of selected representative cells. The images show an overlapping of the cell basic elements with the NP distribution. The table at the bottom of Fig. 9 summarises the quantitative elemental analysis of exposed cells. The intracellular concentrations given in ppm (µg/g) are provided and compared with those of control cells.

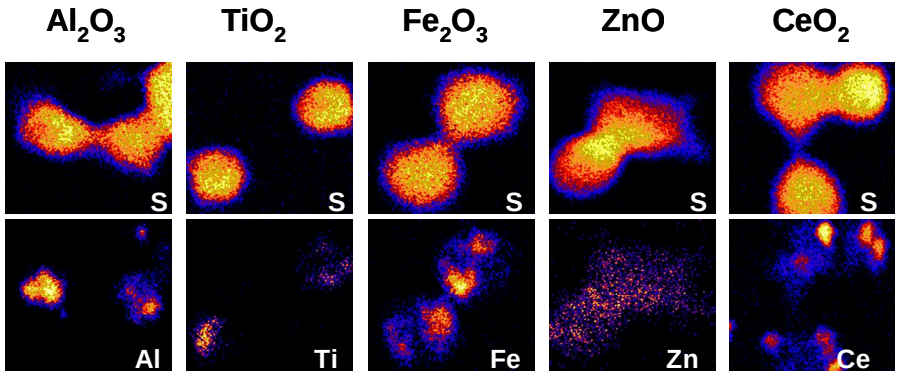

concentration (µg/ml)	30	30	30	30	30
n cells (m experiments)	14(3)	20(3)	10(2)	15(4)	25(8)
treated cells (ppm)	*17900	470	4000	11400	12000
control cells (ppm)	--	--	58	190	--

Fig. 9 PIXE elemental mapping of A 549 cells exposed to different metal oxide NPs at a concentration of 30 µg/ml for 48 h. Top and bottom images demonstrate S and NP related element distributions, respectively. The colour code is as follows: yellow is the maximum while black represents the minimum. The size of all images is 50x50 µm. (*) indicates the correction of the originally measured value by a factor of 1.96 after Aluminium standard calibration. This extra calibration was done because the low PIXE detector efficiency below 2 keV leads to an increase in the error of Al concentration determination

To emphasise the difference between the applied dose and the toxicologically relevant dose, which is the intracellular dose, the term "Genuine Dose" will be used. Dose Exposure-Genuine Dose and Genuine Dose-Toxicity relationships were studied in A549 cells exposed to ZnO and CeO_2 NPs for 48 hours. Results are provided in Fig. 10 and 11. The Genuine Dose and the cytotoxicity were deduced from IBM and MTT experiments, respectively. Cells were treated with bare ZnO and CeO_2 NPs for 48 hours, as well as with surface modified NPs carrying a protein corona. Fig. 10 A and 11 A represent the determined Genuine Doses of the respective NP related elements as a function of the applied dose.

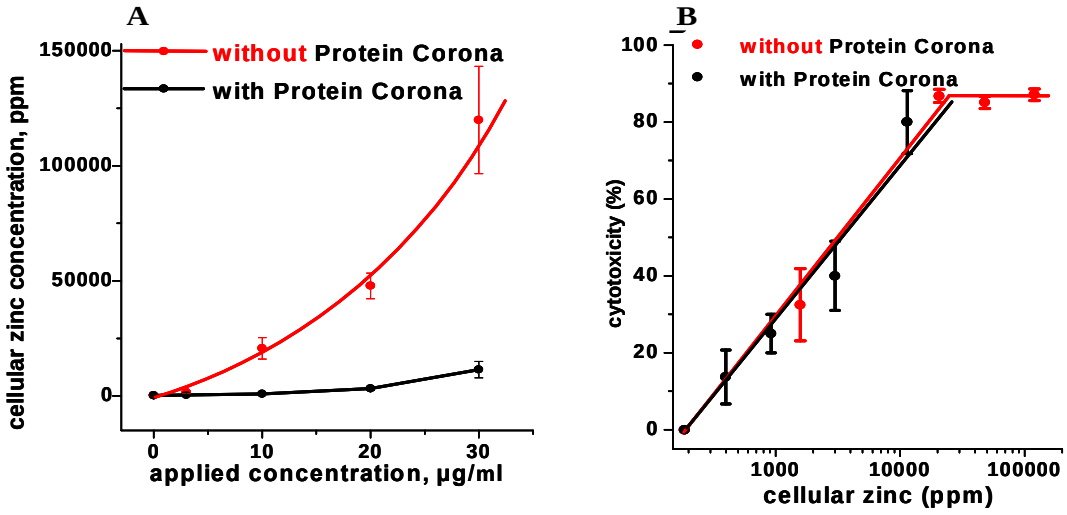

Fig. 10 Exposure-Genuine Dose and Genuine Dose-cytotoxicity relationships of ZnO NPs in A549 cells. A) Uptake as a function of the applied doses for bare and protein corona modified ZnO NPs. B) Cytotoxic cell response as a function of the Genuine Dose for bare and protein corona modified ZnO NPs. The experimental points in B refer to the same applied concentrations as in graph A. The cellular zinc concentration data refer to median values.

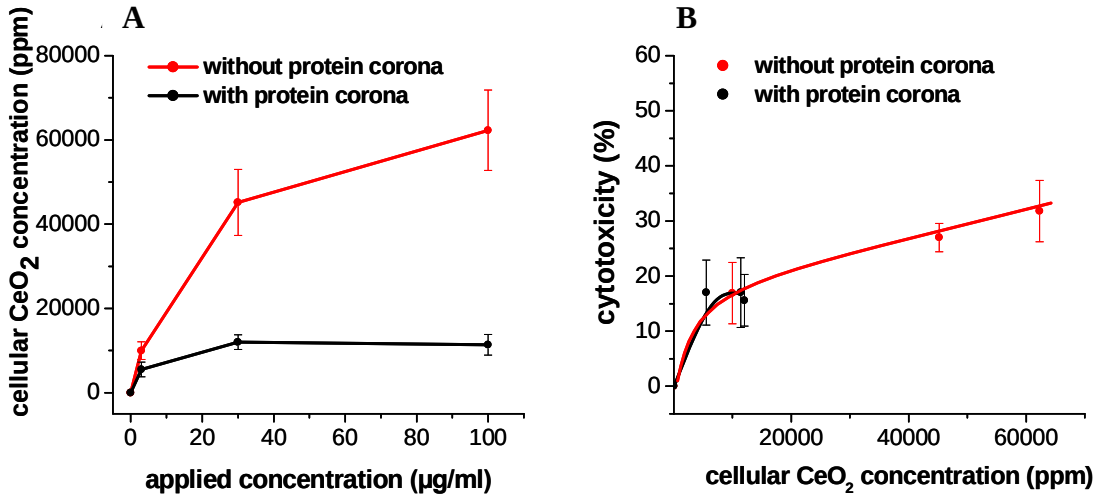

Fig. 11 Exposure-Genuine Dose and Genuine Dose-cytotoxicity relationships of CeO_2 NPs in A549 cells. A) Uptake as a function of the applied doses for bare and protein corona modified CeO_2 NPs. B) Cytotoxic cell response as a function of the Genuine Dose for bare and protein corona modified ZnO NPs. The experimental points in B refer to the same applied concentrations as in graph A. The cellular zinc concentration data refer to median values

Fig. 10 A and Fig. 11 A demonstrate that the Genuine Doses depended strongly on the nature of the surface. NPs without a protein corona were uptaken in much larger quantities than particles with a protein corona. This was observed both for ZnO and CeO_x NPs. In the case of ZnO NPs a trend toward saturation of uptake was not observed at the concentration range used. In the case of CeO_{2-x} NPs there was a trend toward saturation of uptake both for protein modified NPs as well for bare NPs.

Genuine Dose-Toxicity relationships are provided in Figs. 10 B and 11 B for ZnO and CeO_{2-x} NPs. The remarkable finding was that the toxic responses depended only on the Genuine Dose of the respective NPs but not on the nature of the surface of the NP itself. The nature of the surface was thought critical for the uptaken amount of NPs, as shown in Figs. 2 A and 3 A. In the case of ZnO NPs the toxicity reached almost 100%, while there was a saturation trend for CeO_{2-x} NPs.

2.2) NP Internalisation and Distribution Across Treated Cells

Internalisation of NPs was unambiguously detected by analysing the energy spectrum of backscattered protons in the RBS spectrum. Protons penetrate the cell and undergo numerous interactions with the target electrons and nuclei, thereby loosing energy. Therefore, if protons become backscattered from NPs located at a certain depth in the cell, their energy is less than if they would have been backscattered from the cell surface.

Fig. 12 demonstrates an example of an RBS spectrum of a selected cell treated with protein modified Al_2O_3 NPs at a concentration of 30 µg/ml for 48 h. This spectrum is compared with the control RBS spectrum recorded from a thin layer of Al_2O_3 NPs adsorbed onto a polypropylene film. The black arrows denote the energy peaks of protons backscattered from the Al nuclei of three different cells. There is a loss of energy of protons backscattered from Al nuclei proving internalisation of the Al_2O_3 NPs.

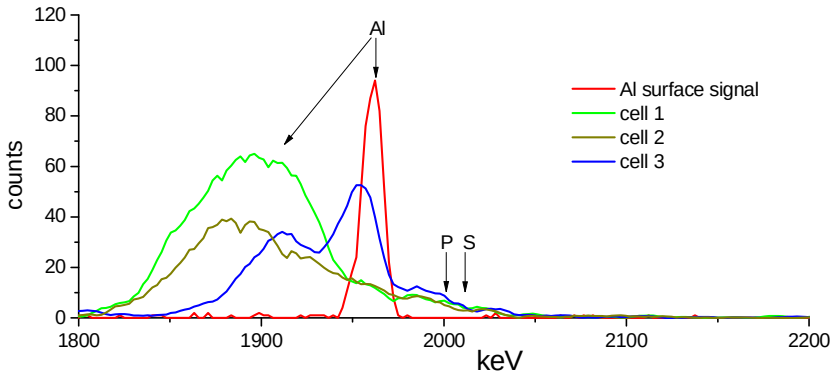

Fig. 12 RBS spectra recorded from three single cells exposed to Al_2O_3 NPs at a concentration of 30 µg/ml for 48 h (green, brown and blue line) and from a dried, thin layer of CeO_2 (red line).

RBS studies with cells exposed to CeO_{2-x} show that they are mostly internalised while ZnO NPs are both internalised and are present on top of the cells.

2.3) Quantification of Intracellular Free Zn^{2+} Ion Concentration

A possible explanation for the observed toxicity of ZnO NP is their degradation, with ion release at low pH. RBS showed that ZnO NPs can be found on the surface of the cell as well as inside, according to the energy displayed by backscattered ions. In order to determine the intracellular concentration of free Zn^{+2} ions flow cytometry experiments were performed employing the intracellular dye FluoZin-3 that binds to free Zn^{+2} forming a fluorescent complex. Fig. 13 A and B provide the intracellular Zn^{2+} ion concentrations as a function of NP exposure and, for comparison, $ZnCl_2$ exposure in the extracellular solution. In both cases a clear correlation can be observed. After exposure to 3 and 10 µg/ml of ZnO NPs, the free Zn^{2+} concentration of the control cells of 1.35 nM was increased to 2.1, and 3.5 nM after 48 h of exposure, respectively. After exposure to 30 µg/ml of ZnO NPs there was a dramatic increase in the intracellular Zn concentration to approximately 200 nM, already beyond the dynamic range of the assay, set by the binding constant of the zinc/FluoZin-3 complex. After 72 h of exposure the increase was similar to that observed after 48 h.

The intracellular concentration of Zn^{2+} was also measured in the presence of increasing concentration of $ZnCl_2$, i.e. increased Zn^{2+} concentration in the media. The results are displayed in Fig. 13 B, here a gradual intracellular Zn ion concentration increase is observed along with a rise in the extracellular concentration. Interestingly, exposure to 200 µm $ZnCl_2$ corresponds approximately to the exposure of the cells to10 µg/ml ZnO NPs.

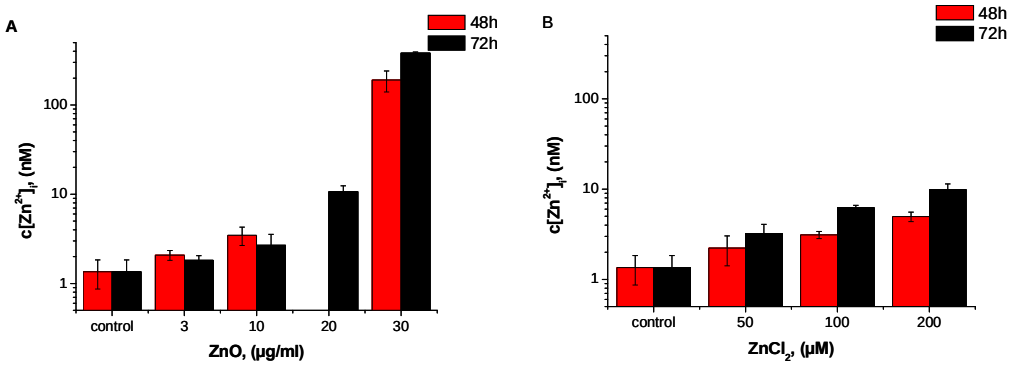

Fig. 13 Intracellular free Zn^{2+}-concentration as a function of ZnO NP concentration and extracellular $ZnCl_2$ concentration. (A) Cells were exposed to different NP concentrations (3, 10, 20, 30 µg/ml) for 48 h or 72 h in RPMI with 10 % FBS (B) Cells were exposed to different $ZnCl_2$ concentrations (50, 100, 200 µM) for 48 h or 72 h in RPMI with 10 % FBS

2.4) NP Uptake, Distribution and Co-Localisation with Cell Components.

CRM allows for studying the distribution and co-localisation of unlabelled NPs inside single cells. Additionally, CeO_{2-x} NPs were fluorescently labelled with RITC and their distribution in A549 cells was studied with CLSM.

Fig. 14 shows Raman images of cell constituents, cell compartments and the NP distribution in a single A549 cell treated with 30 µg/ml CeO_2 NPs for 48 h. The laser beam scans the sample in the xy-plane. Complete Raman spectra were recorded at each pixel. The protein distribution was calculated from the integral intensity of the CH_3 symmetric stretching band (2935 cm^{-1}) and also from the amid III band at 1250 cm^{-1}. Lamellar bodies consisting mainly of lipids were identified from the intensity distribution of the CH_2 symmetric stretching band at 2850 cm^{-1}. The cell nucleus was identified from the integral intensity of the adenine (A) and guanine (G) bands at 1338 cm^{-1}. The CeO_{2-x} NPs display a very strong Raman-active F_{2g} mode at 465 cm^{-1}, related to a symmetrical breathing vibrational bond of O ions around each cation. This band was chosen to map NP distribution in the cell. The confocal plane was chosen in the middle of the cell as derived from a Z-scan.

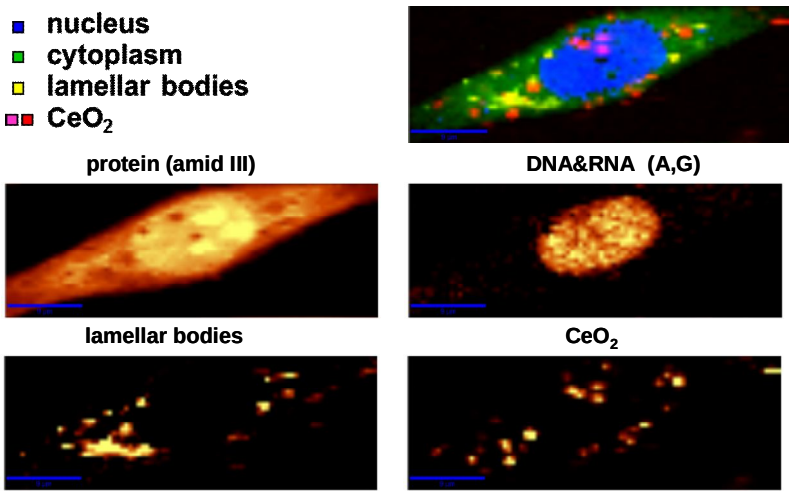

Fig.14 Representative Raman mapping of different cell components as well as NPs in a single A549 cell exposed to 30 µg/ml CeO_2 NPs for 48 h. The image at the top right position represents the overlapping of the four different cell components, nucleus, cytoplasm, lamellar bodies, and CeO_{2-x} NPs. Yellow and black colours of individual

mappings correspond to the maximum and minimum Raman signal intensity respectively. The scale bars denote a distance of 9 µm.

The CLSM technique was applied to monitor the uptake of fluorescently labelled CeO_2 NPs. Results are shown in Fig. 15, A549 cells were exposed to fluorescently-labelled NPs at a concentration of 30 µg/ml for 24 h, with the cell nucleus stained with DAPI.

Fig. 15 shows the uptake of RITC-labelled CeO_{2-x} NPs (red colour) together with the localisation of the nucleus in A549 cells. The NPs can be clearly detected inside the cell by their red fluorescence. As can be seen, the internalised CeO_{2-x} NPs cluster around the nucleus.

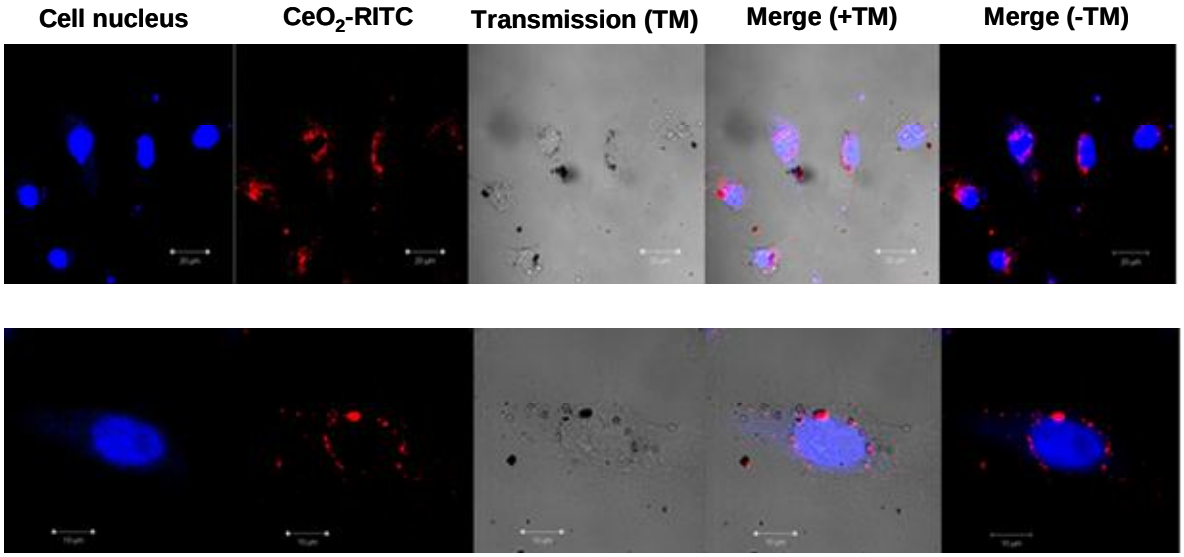

Fig. 15 Uptake of RITC-labelled CeO_2 NPs into A549 cells (30 µg/ml, 24h). The scale bars represent 20 µm.

Both methods demonstrated the uptake of CeO_2 NPs. These findings correlated well with the internalisation data derived from RBS measurements. Furthermore, CRM and CLSM experiments have revealed that CeO_2 NPs become homogeneously distributed forming agglomerates inside cells with a size about 0.5-2 µm. The size and distribution of these agglomerates is similar to a distribution within endosomes/lysosomes. Therefore an endocytotic means of NP uptake is highly likely. CRM images have not shown a co-localisation with the lamellar bodies nor with the nucleus. The CeO_{2-x} NP agglomerates were homogeneously distributed in the cytoplasm. On the contrary, a preferential localisation of CeO_2 NPs adjacent to the nucleus was observed by means of CLSM. The fluorescent dyes present at the particle surface seem to have an impact on the cellular uptake of NPs, their distribution and co-localisation with cell components.

2.5) NP Intracellular Translocation

The intracellular distribution of NPs was studied by means of Transmission Electron Microscopy (TEM) as a function of time. The pattern of uptake and subsequent intracellular traffic was rather similar for CeO_2, Al_2O_3, FeO_x and TiO_x NPs.

Fig. 16 summarises the TEM results regarding the uptake mechanism and intracellular processing. After 4 h most particles are found at the extracellular surface of the cells.

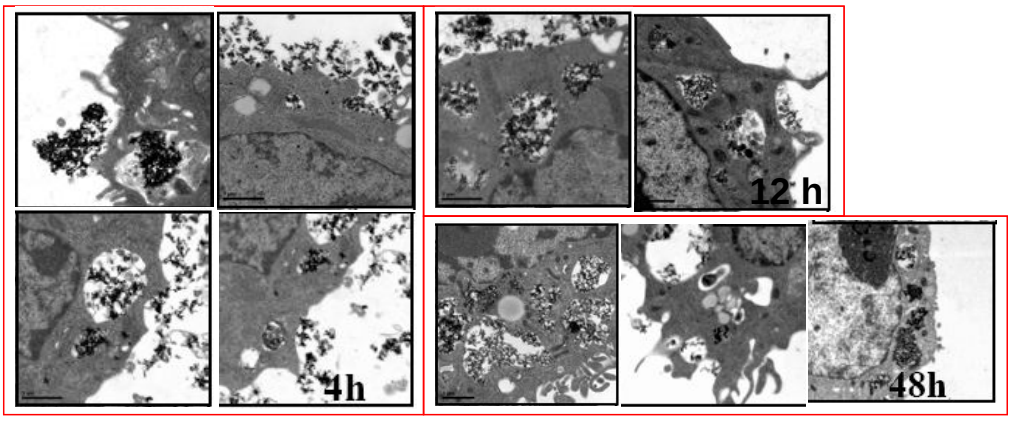

Fig. 16 Transport and intracellular distribution of NPs as a function of time. TEM images demonstrate typical patterns of uptake for CeO_2, Al_2O_3, FeO_x and TiO_x NPs in Raw 264.7 and H460 cells.

The majority of these clusters are in contact with the cell membrane. Many particles became attached to the membrane, and clusters can be observed close to the concave cell membrane, indicating that endocytosis has started. Comparatively few clusters have been already endocytosed.

After 12 h of incubation, the cells have ingested a relatively large amount of the NPs. The NPs appear clearly inside endosomes, as can be inferred from the different staining density of the background. The endosomes have moved together with the NP content towards the nuclear membrane, however, the particles did not penetrate the nucleus.

After 48 h some particles were released into the cytoplasm. The micrograph in the middle has obviously captured an event of exocytosis. Still no particles were found inside the nucleus.

2.6) Interaction of NPs with Proteins and Blood Components

None of the evaluated metal oxide NPs were able to induce complement activation, as the C3 factor remained largely intact, with basal degradation similar to that of the negative control.

The study of the interaction of the metal oxide NPs with plasma protein fractions and high purity albumin, determined by fluorescence and FTIR spectroscopy, shows that the order of the capacity of the NPs to interact with the different fractions and induce protein changes at physiological pH is: $ZnO>>>TiO_2>CeO_2>>Al_2O_3$.

ZnO NPs have a slight denaturising effect, which could explain their high cytotoxicity. The denaturising effect of ZnO NPs was confirmed by studying thermal denaturation of fibrinogen and albumin in the presence of ZnO NPs.

Al_2O_3 NPs were the most inert of the metal oxide NPs tested, and they showed no interaction with any of the protein fractions tested at physiological pH, while CeO_2 NPs only interacted with albumin. This interaction became more intense at basic pH, as determined by FTIR and fluorescence spectroscopy.

When the pH was increased to 8.5, Al_2O_3 NPs were able to interact, but only induced small changes in the protein. At acidic pH, when both the protein and the NPs were positively charged, none of the NPs presented an interaction with albumin. Therefore, when NPs are internalised by cells and enter the endosome, with an acidic pH, the protein corona could be lost or exchanged. The main conformational alteration in albumin upon NP binding was the conversion of an α-helix structure to a β-sheet one, as determined by FTIR spectroscopy.

3) <u>Studies of the Immune Response "in vitro"</u>

The *in vitro* toxicology studies carried out in the HINAMOX project aimed to investigate and compare the cytotoxicity, immunological impact and oxidative stress of different metal oxide NPs. In particular the immune response of cells lines involved in lung injury: Alveolar type II (AT II) cells, lung macrophages and the A549, an immortal cell line of AT II, were studied in order to understand the pathological response of the lung and the role of pulmonary surfactants in the uptake of NPs. Studies on the uptake and immunological response of epithelial lung cells need to be undertaken since these cells also are possible vehicles for the incorporation of NPs, especially during long inhalation processes and the deposition of NPs on lung walls. AT II cells secrete and recycle pulmonary surfactant and contribute to the regeneration of the alveolar epithelium. Alveolar cells, which form the

wall of the alveoli, may be among the first cells to come into contact with inhaled NPs. Therefore alveolar cells will play an important role in NP uptake and processing. AT II pneumocytes (AT II cells) are the pulmonary surfactant producing cells and the progenitors of AT I cells, which primarily make up the alveolar surface.

The mechanical environment of AT II cells was taken into account. AT II cells are continuously exposed to mechanical stresses attributed to changes in the lung volume which result from the in- and outtake of air during the breathing process. Given the nature of breathing, mechanical forces will affect AT II cells in cyclic patterns with variations in cycle frequency and amplitude.

Such breathing patterns can be simulated *in vitro* by cultivating the cells on elastic membranes, with a variable surface area that can be altered by changing the air pressure on the backside of the membranes. With this method, several cyclic breathing patterns, varying in cycle frequency and amplitude were applied on AT II cell cultures during exposure to NPs. The effect of the mechanical environment of AT II cells will be evaluated by comparing cyclically stretched cells with static ones.

Complementary studies on lung macrophages were performed to better elucidate the process of inflammation and to learn what kind of activation is taking place in the presence of NPs: either classically activated, which exhibit a Th1-like phenotype, promoting inflammation (by pro-inflammatory cytokines), or alternatively activated, which exhibit a Th2-like phenotype, promoting cell proliferation and angiogenesis.

Additionally, the immunological response of other cell lines was studied besides the lung. In this way a more general picture of the immunological response towards metal oxide NPs is achieved beyond focusing solely on lung response.

3.1) Lung Cells: AT II and A549 Cell Lines

ZnO NPs have a strong toxic effect on primary AT II and A549 cells, which was determined by Anexin V/Propidium Iodine staining as well as the MTT-conversion assay. AT II cells had been more vulnerable to toxic effects of ZnO than A549 cells. Exposure to ZnO also caused an increase in intracellular ROS generation which might be linked to the toxicity of this kind of NP.

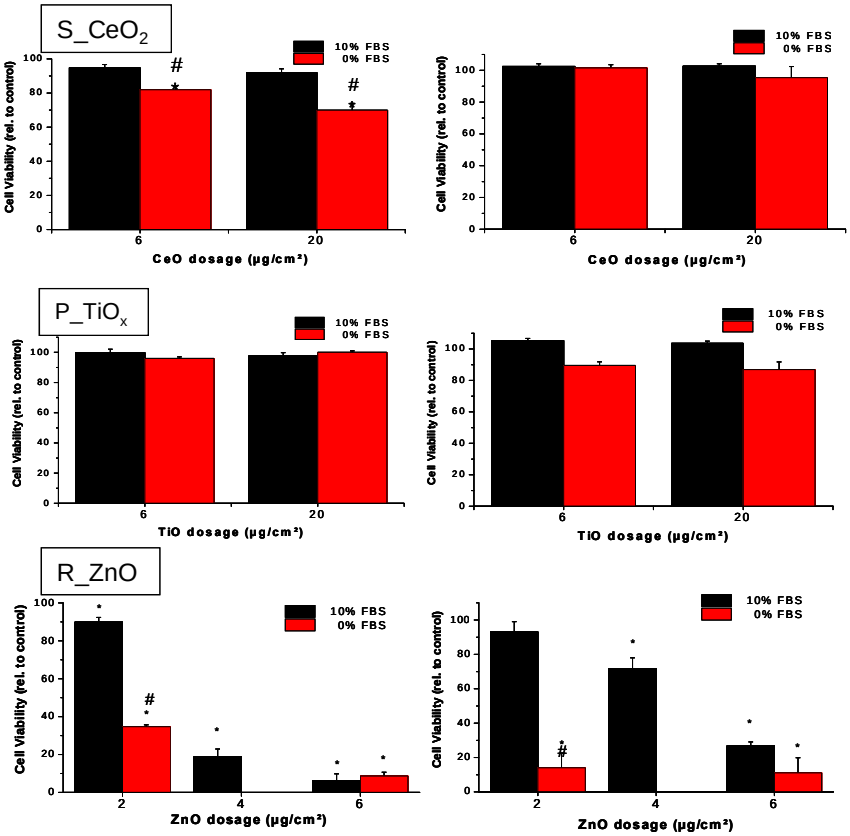

Fig. 17 Cell viability after 24h exposure to metal oxide NP. AT II cells (**left side**) and A549 cells (**right side**) were exposed to different dosages of S_CeO2 (**top**), P_TiOx (**middle**) and R_ZnO (**bottom**) for 24 h. The NP surface was modified with protein corona (**black**) or not modified (**red**) in media containing 10% FBS and 0% FBS respectively. Results were related to controls of the same cell type, which were cultured in the same media type but not to NP. The columns show the means of three independent experiments (± SEM). Asterisks demonstrate significant differences to control cells, whereas # denote significant differences of cells exposed to NP media without FBS to cells exposed to NP media with 10% FBS (student's T-test, $p < 0.05$).

For AT II cells the generation of ROS increased to 147% at a dosage of 4 µg/cm² and 168% at a dosage of 6 µg/cm². This might be one reason for the toxicity of ZnO NPs, since both dosages were toxic for AT II cells as well. This presumption was re-enforced by the fact that a dosage of 2 µg/cm² of ZnO NPs, which was not toxic for AT II cells, also caused no significant increase of ROS generation. Contrary to AT II cells, the ROS generation in A549 cells increased slightly at a ZnO NP dosage of 6 µg/cm², showing that A549 cells seemed to be more resistant to adverse effects due to exposure to ZnO NPs, as was also demonstrated in the viability measurements.

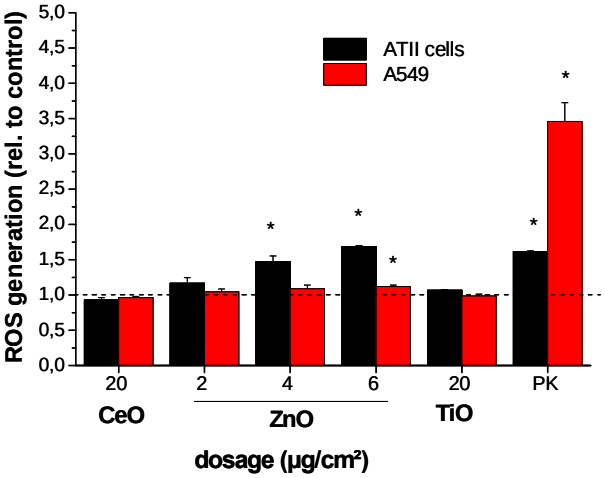

Fig. 18 Intracellular generation of ROS as an indicator of oxidative stress in cells exposed to metal oxide NP. AT II cells (**black**) and A549 cells (**red**) were exposed to S_CeO, P_TiO (both: 20 µg/cm²) and ZnO NPs (2, 4, 6 µg/cm²) in culture medium with FBS (10%) for 4 h (AT II cells) resp. 6 h (A540 cells). The intracellular ROS generation was determined by staining the cells with CM-H2DCFDA, which becomes a fluorescent dye by reacting with ROS. The fluorescent intensity was measured by flow cytometry. 200 µM H_2O_2 (AT II cells) and 500 µM H_2O_2 (A549) were used as a positive control (PK). Results are calculated in relation to control cells, which were stained with the same dye but not exposed to NPs. The columns show the mean value of at least three independent measurements (± SEM). Asterisks denote significant differences to control cells of the same type (student's t-test, $p < 0.05$).

Crucial for the toxicity of ZnO was the release of Zn^{2+}, since the more stable _ZnO NPs doped with Mg, which released less amounts of Zn^{2+}, were not as toxic as ZnO NPs.

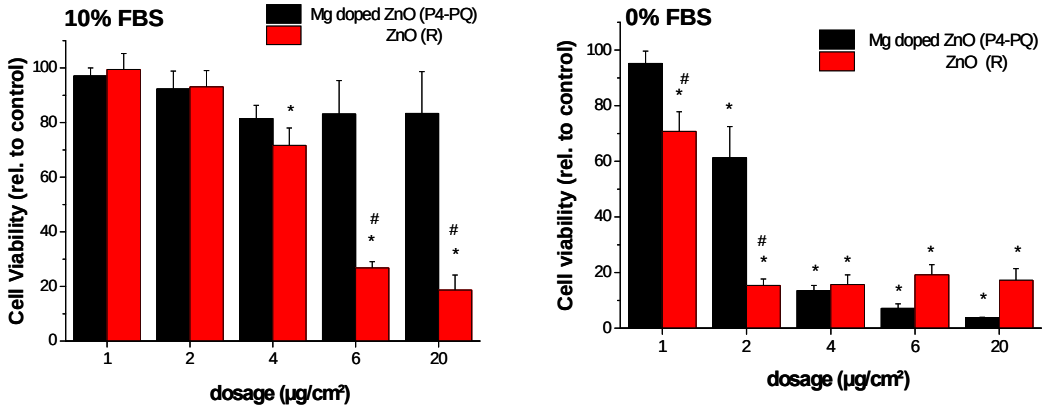

Fig. 19 Effect of Mg doped ZnO on the cell viability of A549 cells compared to the effects of R_ZnO. A549 cells were exposed to different dosages (1, 2, 4, 6, 20 µg/cm²) of the P4-PQ_ZnO-Mg (**black**) and R_ZnO (**red**) for 24 h. The exposure media contains 10% FBS (**top**) or no FBS (**bottom**). Cell viability was determined by using the MTT conversion assay. Results are calculated in relation to control cells. The columns show the mean value of three independent experiments (± SEM). Asterisks show significant differences to control cells, whereas # denote significant differences between the effects of ZnO to the effects of P4-PQ_ZnO-Mg (student's t-test, $p < 0.05$).

A similar conclusion was reached when the ZnO NPs were surface modified with a silane. The silane modification made them more stable and toxicity was therefore reduced.

Exposure to CeO_2 and TiO_x NPs had not reduced the viability of both cell types. The exposure of cells to CeO_2 and TiO_x NPs did not affect the ROS generation.AT II and A549 cells, exposed to ZnO NPs, released higher amounts of MIP-2. MIP-2 is a chemokine that recruits neutrophils into tissues and is therefore related to an acute inflammation. Furthermore, an increase in the release of TNF-α and eotaxin-1 by A549 cells was determined, indicating an amplification of the inflammation and the recruitment of Eosinophils. The pro-inflammatory potential of ZnO NP is linked to the toxicity of this NP, since only toxic dosages of ZnO NPs caused an increase in the release of cytokines.

For these studies the NPs were suspended in FBS to coat them with a protein corona and reduce aggregation following a protocol developed within the consortium. NPs suspended in cell media without a protein corona, tend to form much larger, polydisperse aggregates and exhibit higher toxicity, which was especially true for ZnO NPs. This effect might be related to higher uptake rates of such prepared NPs, which could have been demonstrated for CeO_2 NPs by flow cytometric side scatter (SSC) measurements.

3.2) Breathing Patterns in AT II Primary Cultures

The application of breathing patterns reduced the toxicity of ZnO NPs. This reduction was most evident in a heavy breathing pattern, which used the highest cycle amplitude. This might be due to a reduced uptake of NPs by stretched AT II cells. This was indicated by the fact that the application of breathing patterns had reduced the uptake of transferrin as well as CeO_2 NPs as measured by SSC and PIXE. Since transferrin is a marker for the clathrin-mediated endocytosis, these results indicate that this kind of endocytosis is affected by the application of breathing patterns. In AT II cells, the clathrin-mediated endocytosis is also related to the surfactant recycling and might be one major route of entry for CeO_2 NPs and probably for other NPs.

ROS generation in AT II cells by ZnO NPs was reduced when breathing patterns were applied. These results can be linked to the reduced toxicity of ZnO NPs for cyclically stretched AT II cell cultures. For CeO_2 NPs, the intensity of ROS generation was reduced to 88% (± 3%) at a dosage of 20 µg/cm² and to 86% (± 8%) at a dosage of 40 µg/cm² in relation to control cells. For the heavy breathing pattern, a significant reduction of ROS was only observed at a dosage of 20 µg/cm² (91% ± 2%). In these cases, CeO_2 NPs seemed to have an antioxidant effect decreasing ROS generation. In static conditions no significant variation in ROS generation could be observed in the presence of CeO_2 NPs in relation to control cells. TiO_x NPs had no significant effect on the intracellular ROS generation in AT II cells, in this case ROS is seen to be independent of the administered dosage or applied breathing pattern.

The application of breathing patterns on AT II cells during exposure to ZnO NPs reduced the amount of released MIP-2 as it also reduced the toxicity of NPs. In a heavy breathing pattern, the amount of released MIP-2 was not higher than control cells. The application of breathing patterns slightly inhibited the clathrin-mediated endocytosis, which may be a major uptake route of NPs. Therefore the pro-inflammatory potency of NPs might be related to their uptake efficiency by epithelial cells.

CeO_2 and TiO_x NPs did not induce an increased release of cytokines in either AT II or A549 cells, independently of applied breathing patterns and seem to exhibit no pro-inflammatory potency on lung tissue.

3.3) Cell Viability and Immune Response in Other Cell Lines

Toxicity assays performed in the human tumoral cell lines A549, NCI-H460, SK-MES-1, HeLa and Jurkat using colorimetric and electric cell viability tests showed that only ZnO NPs are toxic. Other NPs under investigation did not reduce cell viability significantly enough to be considered toxic as well.

Despite most of the metal oxide NPs studied being non-toxic they are not necessarily inert in their interaction with cells. It was observed that NPs can alter the different activation cell pathways and induce cytokine production.

The MAPK/ERK pathway that is related to cell growth or uncontrolled cell growth (cancer) was first studied. CeO_2 and TiO_2 NPs induce differential activation of ERK in the Jurkat cell line depending on the pre-stimulation of the cells with PHA or the lack of pre-stimulation. These NPs activate also p38, but only in pre-stimulated lymphocytes. However, TiO_2 NPs but not CeO_2 NPs activate the NFκB pathway. ZnO NPs activate the three MAPKs studied (ERK, p38 and SAP/JNK) in Jurkat, independently of the pre-stimulation with PHA. Al_2O_3 NPs activate only ERK in pre-stimulated lymphocytes, but they seem to induce also NFκB, in agreement with the release of the pro-inflammatory cytokine IL-8. In NCI-H460 cells, a pulmonary cell line, only ZnO NPs are able to activate the three MAPKs. Nonetheless, ZnO and Al_2O_3 NPs activate also the NFκB pathway, indicating that these NPs cause the most inflammatory reaction amongst the four metal oxide NPs studied in the activation pathway experiments.

CeO_2 and TiO_2 NPs are more inert in the pulmonary cell line compared with the lymphocyte cell line, although the activation of p38 depends on lymphocyte pre-stimulation. TiO_2 NPs activate NFκB in Jurkat but not in NCI-H460, although the activation in this cell line could be delayed, since a single experiment done after 6 hours suggests a decrease in IKBα, the NFκB inhibitor.

Gene expression studies in Jurkat cell line incubated with ZnO, CeO_2 or TiO_2 NPs using qPCR showed that NPs alter the expression of some genes related to the cell cycle.

There is also activation of some genes related to cell growth and antiapoptotic genes for CeO_2 NPs, in agreement with the proliferative properties attributed to these NPs. For TiO_2 NPs, the expression of genes related with inflammation was also detected and for ZnO NPs there was activation of some genes implicated in apoptosis, in agreement with the cytotoxic potential of these NPs.

ZnO and Al_2O_3 NPs induce the release of IL-8, a potent chemoattractant cytokine, in PBMCs from all the donors tested. Moreover, ZnO NPs induce the release of IL-6, a pro-inflammatory cytokine. CeO_2 NPs induce the release of some cytokines but only at low concentrations and only in some of the donors tested, in agreement with the low inflammatory potential determined by other techniques (qPCR). Interestingly, TiO_2 NPs have shown negative results for all the cytokines tested while still being able to activate the inflammatory NFκB pathway in Jurkat as detected by performing a western blot, and to activate some genes related with inflammation as seen by qPCR. Nevertheless, detection of IL-4 mRNA up-regulation was seen in the qPCR studies.

The studies of integrin expression variation in Jurkat cells incubated with different metal oxide NPs have shown that all of them induce some alteration in these surface molecules (increasing or decreasing the protein level), and most of the cases are dose-independent. Al_2O_3 NPs up-regulate CD62L and CD184. The up-regulation of both integrins could alter the adhesion profile of the lymphocytes in the presence of Al_2O_3 NPs.

4) Biodistribution, Biological Fate and Quantification of NPs "in vivo"

A fundamental part of the work in the HINAMOX project was the study of the biological fate of metal oxide NPs in animal models following different exposure routes: oral, inhalation, topical and intravenous. For this work NPs were radiolabelled. Positron Emission Tomography (PET) was employed for the visualisation of the NPs in male rats using an eXploreVista-CT small animal PET-CT system. The distribution of NPs in the animals was monitored over time. Activity could be measured per organ obtaining a quantification of the relative NP distribution in the body.

4.1) Biodistribution of ^{13}N-Radiolabelled NPs

^{13}N labelled Al_2O_3 NPs with a short half life, generated after direct activation of NPs provided by PlasmaChem were first employed to visualise the biodistribution of NPs shortly after delivery. Biodistribution studies showed a

strong size dependency of the distribution and accumulation of NPs in all organs. NP uptake, expressed as % of injected dose per organ, is shown in Fig. 20 A–D.

After I.V. injection, a high proportion of the NPs (≈25% for NS_{40nm} and NS_{150nm},, ≈20% for $NS_{10\mu m}$) was rapidly accumulated in the liver irrespective of particle size. Although retention in the liver should be favoured in larger NPs due to phagocytises. The lower uptake observed for $NS_{10\mu m}$ with respect to NS_{40nm} and NS_{150nm} might be due to the higher uptake of $NS_{10\mu m}$ in the lungs (see below) which decreases the bioavailability of these NPs.

Very low accumulation (<2%) of NPs, probably attributable to the contribution of NPs in blood or to spontaneous aggregation, was observed in the lungs for NS_{40nm} NPs. Higher accumulation in the lungs was observed when larger NPs were administered. Values around 7% and 15% (NS_{150nm} and $NS_{10\mu m}$ NPs, respectively) were found. The high values obtained for $NS_{10\mu m}$ particles points strongly to NP trapping in capillary pulmonary bed by size exclusion; however, engulfing by phagocytic cells cannot be discarded.

The accumulation of radioactivity detected in the kidneys and in the bladder suggests a slow elimination of the NPs via urine for smaller NPs (NS_{40nm}). Low accumulation for larger particles might be explained by the high trapping in the lungs due to size exclusion and in other organs by trapping in the RES which decreases the amount of available NPs for urinary excretion.

Accumulation of NPs in the brain was negligible irrespective of NP size.

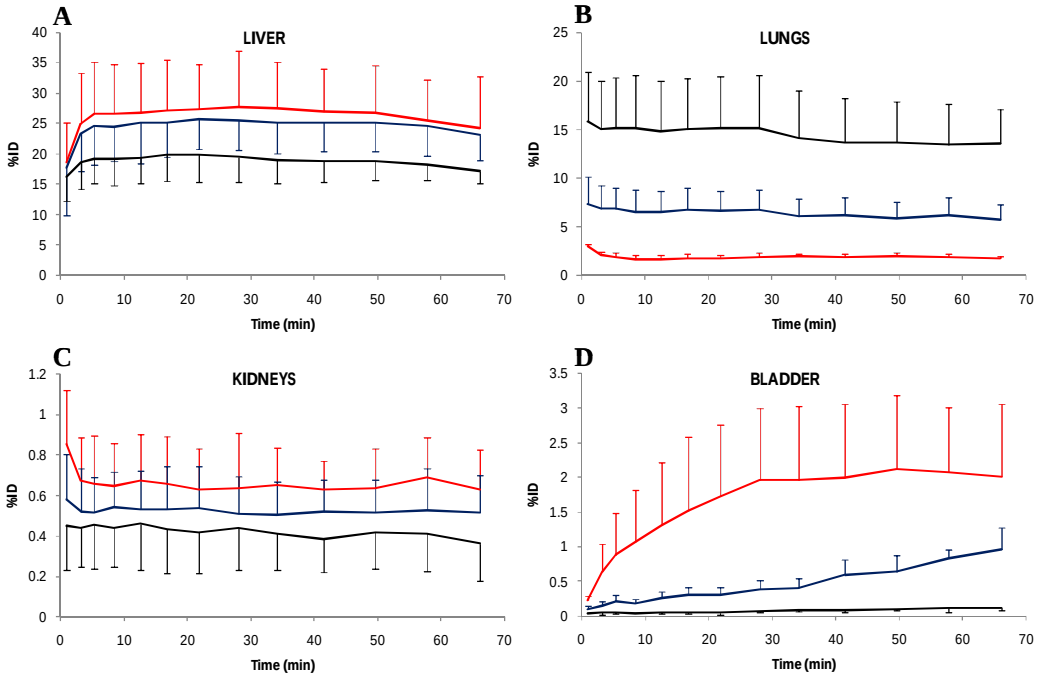

Fig. 20 Time activity curves in different organs, expressed as percentage of injected dose per organ, for different particle sizes: NS_{40nm} NPs (red), NS_{150nm} NPs (blue) and $NS_{10\mu m}$ NPs (black).

4.2) Biodistribution of ^{18}F-Radiolabelled NPs

The use ^{18}F-radiolabelled NPs synthesised exclusively for biodistribution studies allowed for visualisation of the NPs for longer times when compared to ^{13}N labelled NPs generated after activation of the commercial NPs produced by PlasmaChem.

4.2.1) Intravenous administration

Irradiated ^{18}O-enriched metal oxide NPs with no further modification were used to assess biodistribution patterns in animals using PET-CT in male rats after IV administration.

4.2.1.1) Al_2O_3 NPs

The biodistribution pattern at different times post-administration is shown in Fig.21. Most of the radioactivity accumulated in the liver even at very short times. Radioactivity was also detected in the lungs, heart, kidneys, spleen and stomach. The detection of radioactivity in the heart at long times after administration suggests slow elimination of the NPs from the bloodstream while the significant uptake in the bladder, even at times shortly after administration, confirms elimination via urine. Accumulation of radioactivity in the brain and in the testicles was very low, while accumulation in the bones was low but detectable. Sodium ^{18}F-fluoride is a well known PET tracer used for detection of skeletal abnormalities and its uptake reflects blood flow and bone remodelling. The accumulation detected here suggests a potentially very slow leakage of [^{18}F]F^- from the NPs, although direct NP uptake cannot be discounted.

4.2.1.2) TiO_2 NPs

The biodistribution pattern at different times post-administration is shown in Fig.22. As can be seen in the figure, a very similar pattern to the one obtained for Al_2O_3 NPs was obtained. Most of the radioactivity accumulated in the liver; radioactivity was also detected in low amounts in the lungs, heart and kidneys. The significant uptake in the bladder confirms elimination mainly via urine. Accumulation of radioactivity in the bones was low but detectable, suggesting a potentially very slow leakage of [^{18}F]F^- from the NPs, although direct NP uptake cannot be discounted. Significant accumulation was also detected in the gastro-intestinal track, especially at long times after administration of the NPs.

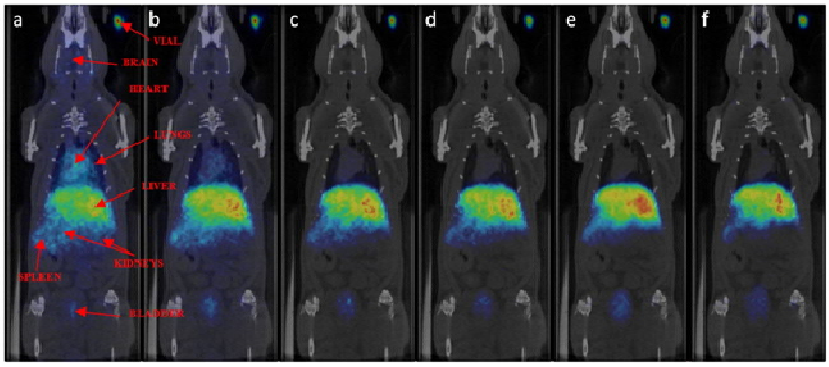

Fig. 21 PET images of ^{18}F-labelled Al_2O_3 NPs obtained at different time points: 0-4 min (**a**), 5-8 min (**b**), 9-12 min (**c**), 13-16 min (**d**), 60-80 min (**e**) and 409-465 min (**f**) after IV injection. PET coronal projections show different tracer distribution over time. CT images were adjusted along the Y axis at each time point for an appropriate fitting with the tracer distribution image in both cases. A small vial containing 3 µL of the NPs solution was simultaneously scanned for determination of the decay curve.

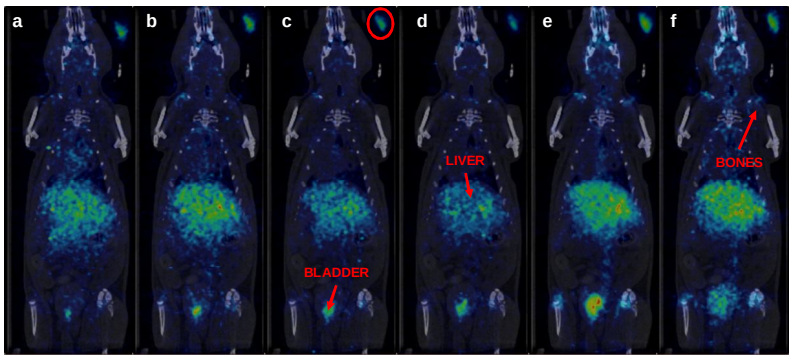

Fig. 22 PET images of ^{18}F-labelled TiO_2 NP obtained at different time points: 0-4 min (**a**), 5-8 min (**b**), 9-12 min (**c**), 13-16 min (**d**), 60-80 min (**e**) and 409-465 min (**f**) after IV injection. PET coronal projections show different tracer distribution over time. CT images were adjusted as in Fig 21. A small vial containing 3 µL of the NPs solution was simultaneously scanned for determination of the decay curve.

4.2.1.3) ZnO NPs

The biodistribution pattern at different times post-administration is shown in Fig. 23. A very different pattern was observed in this case, with accumulations mainly in the kidneys, bladder, and in the bones. These results suggest that ZnO NPs are quickly dissolved after administration, with subsequent release of $^{18}F^-$ which accumulates in the bones and is eliminated via urine.

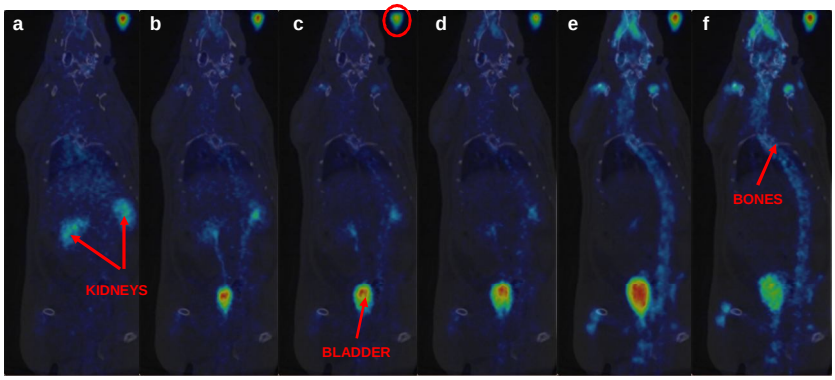

Fig. 23 Positron emission tomography (PET) images of ^{18}F-labelled ZnO NP signal at different time points: 0-4 min (**a**), 5-8 min (**b**), 9-12 min (**c**), 13-16 min (**d**), 60-80 min (**e**) and 409-465 min (**f**) after IV injection. PET coronal projections show different tracer distribution over time. Computerised Tomography (CT) images were adjusted along the Y axis at each time point for an appropriate fitting with the tracer distribution image in both cases. A small vial containing 3 µL of the NPs solution was simultaneously scanned for determination of the decay curve.

Fig.24 shows time activity curves for the three types of NPs in the liver and bones. The differences in the biodistribution pattern mentioned above can be clearly seen.

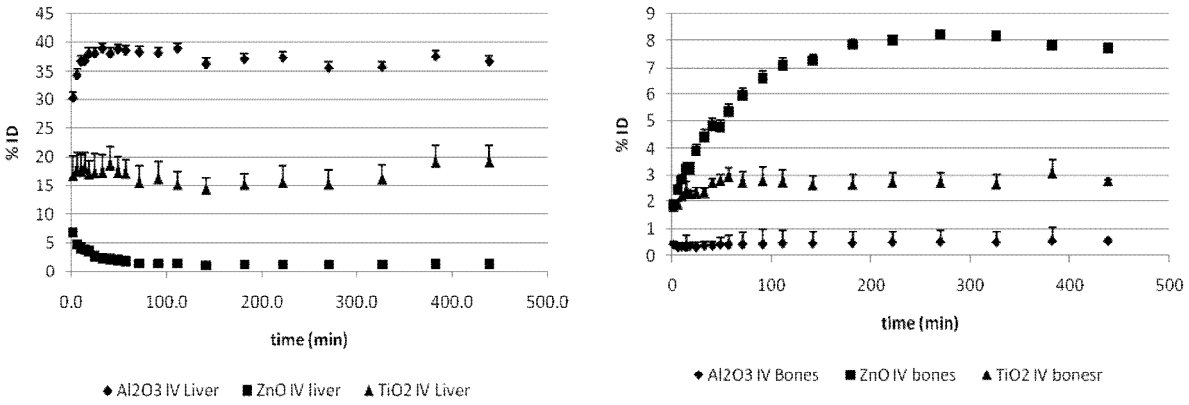

Fig. 24 Time activity curves for the liver (left) and bones (right) as determined by PET using Al_2O_3, ZnO and TiO_2 NPs labelled with ^{18}F.

4.2.2) Oral Administration

For all NPs, a very high percentage of orally administrated NPs (>90%) remained in the stomach, oesophagus and intestine throughout the duration of the study (see Fig.25. The high accumulation of radioactivity in these areas hampered the determination of accumulation in other organs. However, small amounts of radioactivity could be detected in the bladder for TiO_2 NPs.

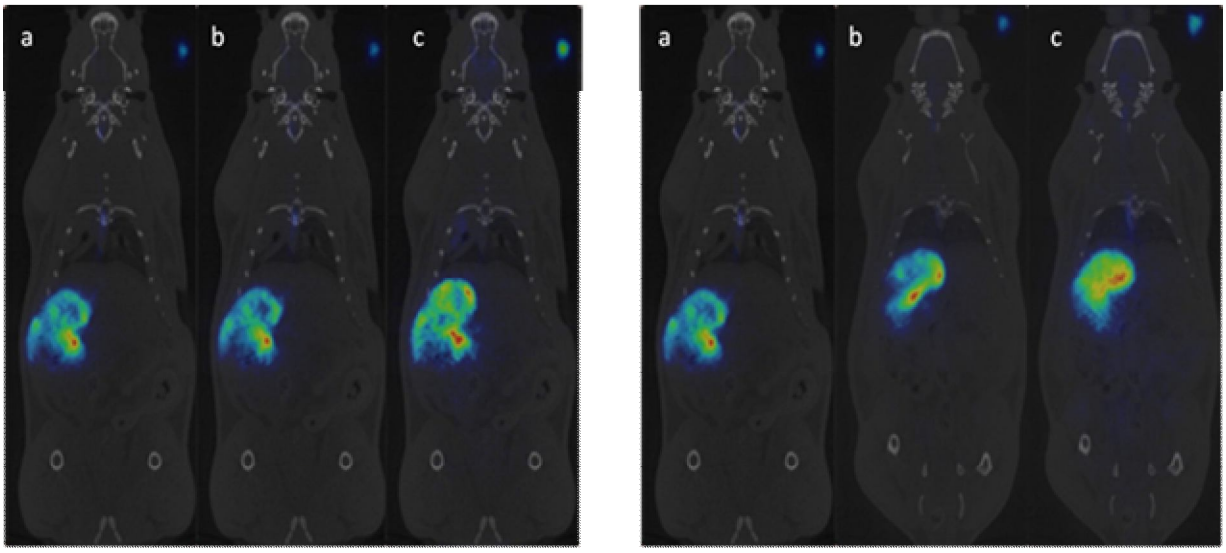

Fig. 25 Images for Aluminum oxide (left) and zinc oxide (right) NPs after oral administration at time: a) 0-4 minutes, b) 5-8 minutes and c) 6,8-7,2 hours.

4.2.3) Topical Administration

No penetration through the skin was detected for any of the NPs studied and all radioactivity was found at the administration point throughout the duration of the study (Fig. 26). These results suggest that penetration of NPs through the skin is a very slow process; thus, the labelled NPs developed in the framework of this project are not suitable for tracking this process.

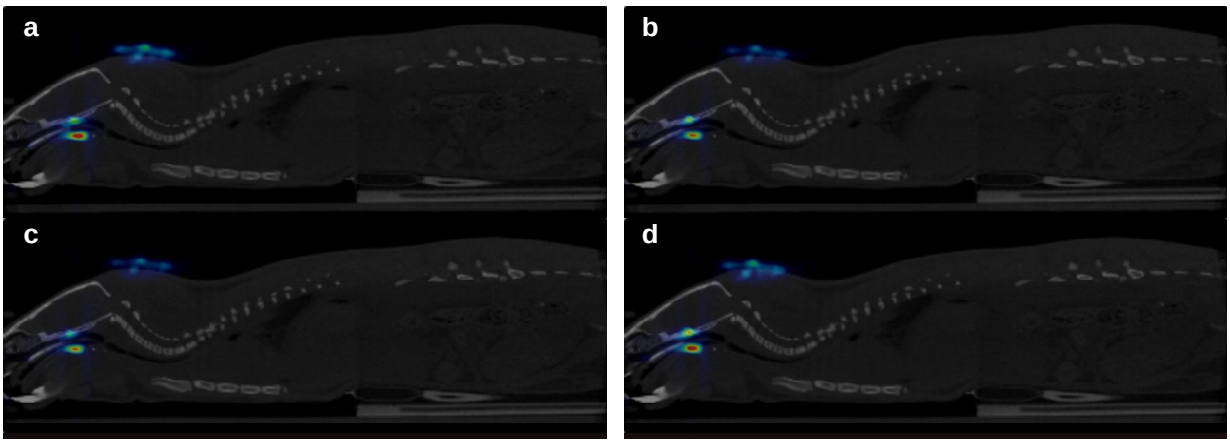

Fig. 26 Images for Aluminum oxide NPs after topical administration at time: a) 0-4 minutes, b) 5-8 minutes and c) 60-80 minutes and d) 410-465 minutes.

4.2.4) Inhalation

Inhalation studies were performed only with Al_2O_3 NPs via irradiated ^{18}O-enriched aluminium oxide NPs. After the irradiation process, the radioactive NPs were introduced into a specially designed inhalation chamber (Fig. 27). Rats were placed in a small glass chamber connected directly to the main chamber. By activation of a speaker at a predetermined frequency, a cloud of NPs was generated and animals were exposed for 15 minutes.

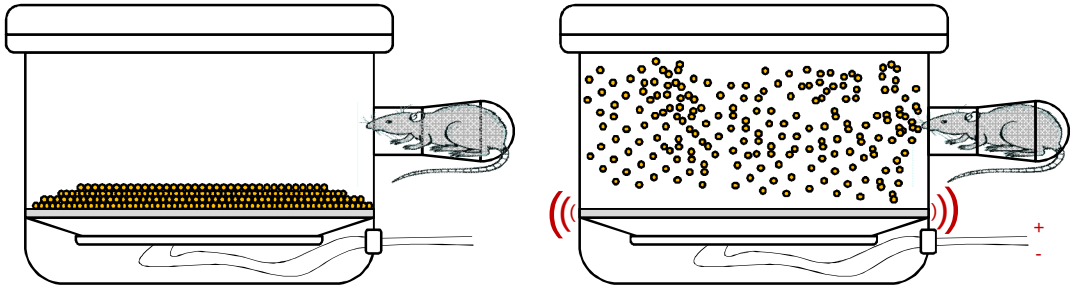

Fig. 27 Specially designed chamber for NP inhalation studies. The NPs were introduced into the chamber while rats were placed in a small glass chamber connected directly to the main chamber (left). By activation of a speaker, a cloud of NPs was generated and animals were exposed for 15 minutes (right).

After different exposure times, animals were sacrificed, the organs removed and the amount of radioactivity determined with a gamma counter. Most of the radioactivity was found in the gastro-intestinal track, including the intestine and stomach (Fig. 28). Significant amounts of radioactivity were also found in the lungs and bladder, the latter increasing with time. Activity in other organs, although detectable, was not significant.

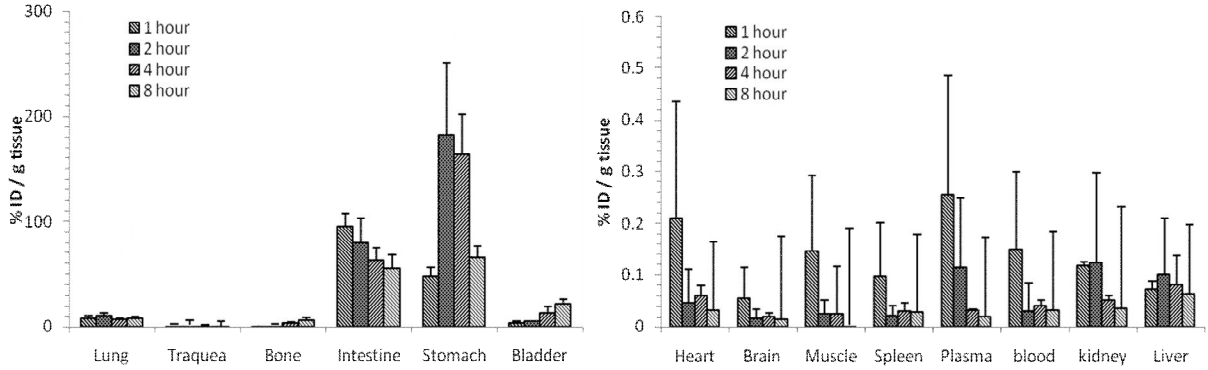

Fig. 28 Amount of radioactivity in different organs as determined by gamma counting.

4.3) Inflammation studies

For the assessment of the inflammatory effect of ZnO NPs in the lungs after inhalation, commercially available NPs were used. Animals were exposed to NPs for 1 hour in a chamber similar to that shown in Figure 27. At t=1, 7 and 28 days after initial exposure, animals were scanned with the PET using [^{18}F]FDGas marker.

Time-activity curves in the lungs were obtained from PET-CT images (Fig. 29 a); a volume of interest (VOI) was also drawn in the cavity of the myocardium to obtain the blood input function (Fig. 29 b), which was corrected by true blood radioactivity measurements obtained from blood samples drawn during scans (Fig. 29 c).

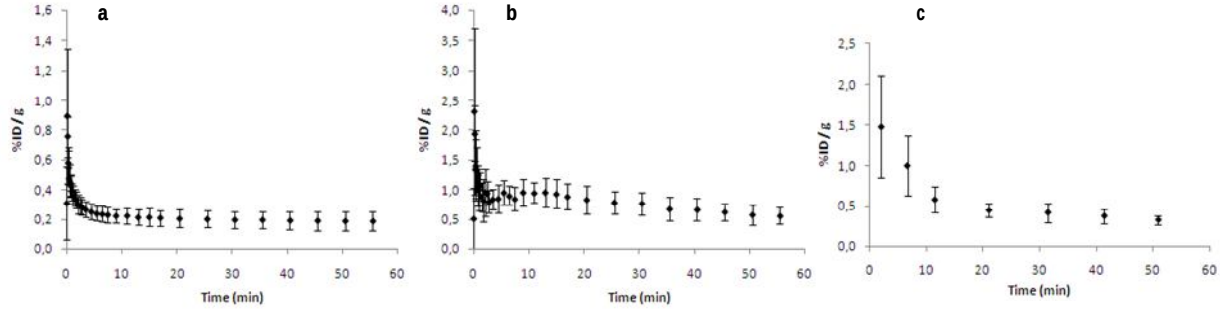

Fig. 29 Time activity curves (as %ID/g) derived from image quantification. Curves corresponding to uptake in the lungs (a), and blood (b); Blood input function derived from blood samples drawn during scans is shown in (c). Average curves for animals exposed to ZnO NPs at t=1day are presented (average ± standard deviation, n=6).

Time activity curves were analysed using the Patlak graphical analysis (Fig. 30 a). In this analysis, the slope of the linear range is proportional to the uptake ratio of [^{18}F]FDG, which can be correlated with the presence of

neutrophils, cells that are known to require high doses of glucose. A high value for the slope (0.00174) was obtained for the animals subjected to NP inhalation at t=1 day after exposure, suggesting the presence of an inflammatory response. This value dropped to 0.00042 (the same level obtained for control animals) at day 7, suggesting a progressive recovery of the animals (Fig. 30b and 31).

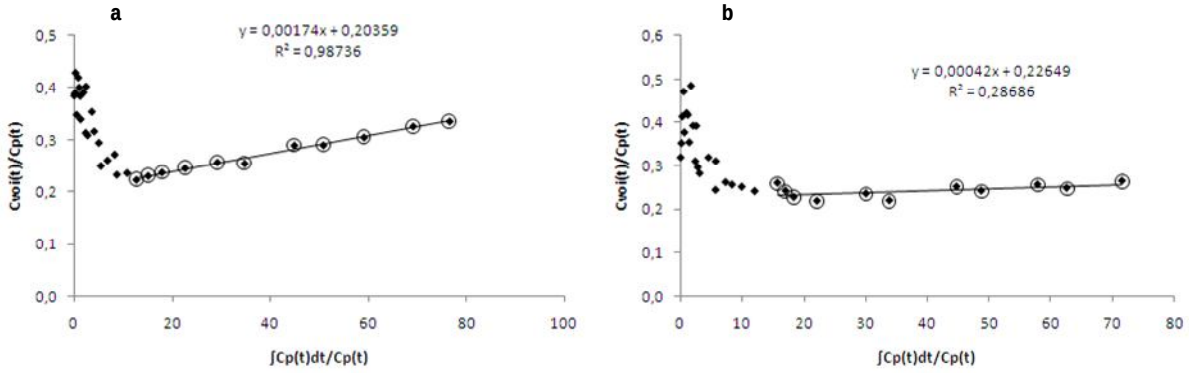

Fig. 30 Patlak graphical analysis corresponding to animals exposed to ZnO NPs at t=1day (a) and t=7 days (b) after exposure.

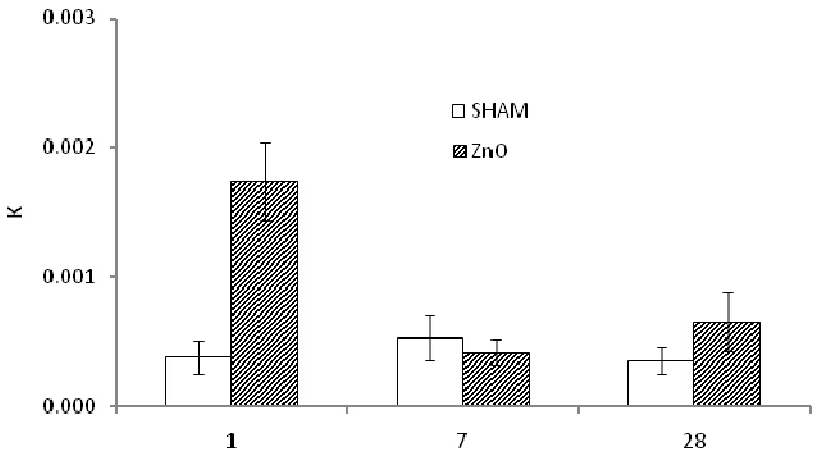

Fig. 31 Slope obtained from Patlak analysis for control and exposed animals at different times after exposure to NPs.

To corroborate the presence of an inflammatory response, inmunofluorescence assays were performed on the lungs of exposed and control animals. The images obtained revealed high infiltration of neutrophils at day one in exposed animals (Fig. 32 a and 32 b). The presence of neutrophils could not be detected in the control animals (Fig. 32 c and 32 d) and in exposed animals at longer times after exposure.

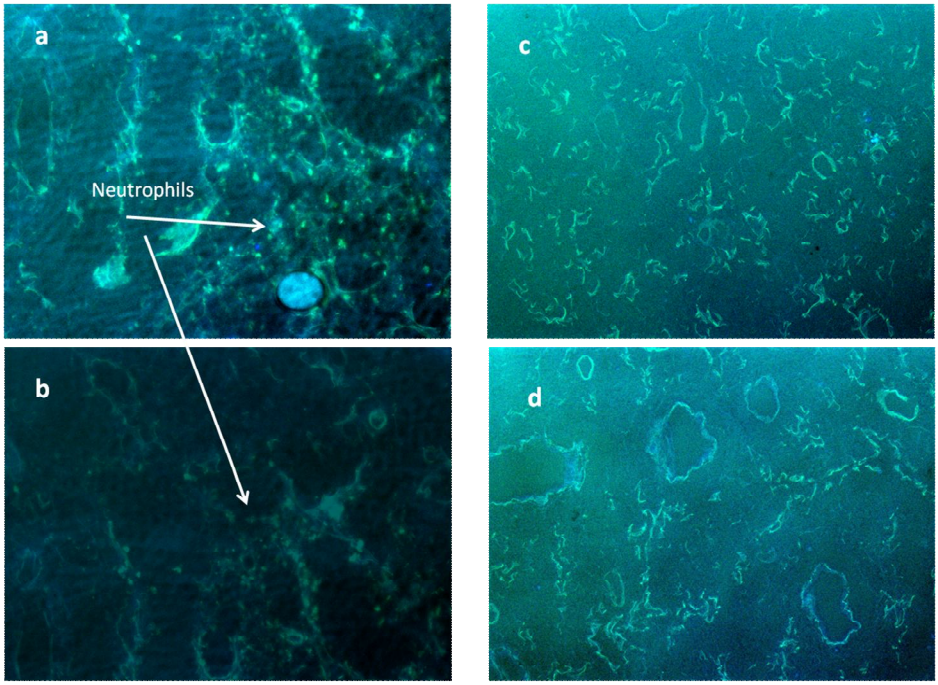

Fig. 32 Inmunofluorescence analysis of the lungs of exposed (a, b) and control (c, d) animals. The presence of neutrophils could be detected only in exposed animals.

5) Dustiness and NP Concentration during Production and Handling of Metal Oxide NPs

The concentration and dustiness of metal oxide NPs in the air during production and handling of the selected NPs were studied as an assessment tool for immediate associated health risks.

5.1) Dustiness of NPs

Standard dustiness tests reveal that two powders of NPs can be categorised as being not highly dusty powders: TiO_2 and Al_2O_3NPs can be considered as very low. The rest of the powders lay in the category of highly dusty powders. In general, increases in humidity caused a decrease in dustiness. The effect of pressure load was more ambiguous. Almost every tested powder responded very differently to the different kind of parameters involved. The different behaviour may be due to differences in their physical state, such as primary particle size, degree of agglomeration and aggregation, coating/stabilising agents etc. As typically observed for dusts from NP powders, there were major size-modes with a peak around 200 nm and a multimodal size-distribution with several size-modes in the particle size distribution greater than 1 µm. Samples of CeO_2, ZnO and TiO_2 NPs also had size modes in the smaller nano-range (<100 nm). Generally, all pressure loadings show a reduction in coarser particles at 30 and 50% Relative Humidity (RH). The only exception was observed for TiO_2 NPs. At 70% RH three of the powders (Al_2O_3, CeO_2 and ZnO) show an unaltered behaviour due to pressure loading in this region.

The exposure modelling was completed for four different work activities: 1) Scooping powder, 2) Wet mixing, 3) Pouring/Bagging, and 4) Dry Mixing (continuous feed via a tube). The amounts of handled nanomaterials varied from 100 g to 10 kg. The duration of the activity/process was from fifty minutes to several hours.

The results from modelling showed that there is a large variation in the potential exposure level depending on both the material and the process (the type and mass-flow in process). The bagging (scoop/filling) and wet mixing scenarios were the simulated work scenarios that resulted in the highest acute exposure risk. Modelling results showed that there is a risk of NP exposure associated with the various handling scenarios tested. One powder, TiO_2 NPs, has a very low dustiness index and hence results in a very low potential of exposure. The risk of exposure is mostly related to acute exposure induced by short-term peaks in the near-field occurring during the activities. According to the modelling, the exposure level of work-day exposure to NPs may be low in the far-field (the general workplace).

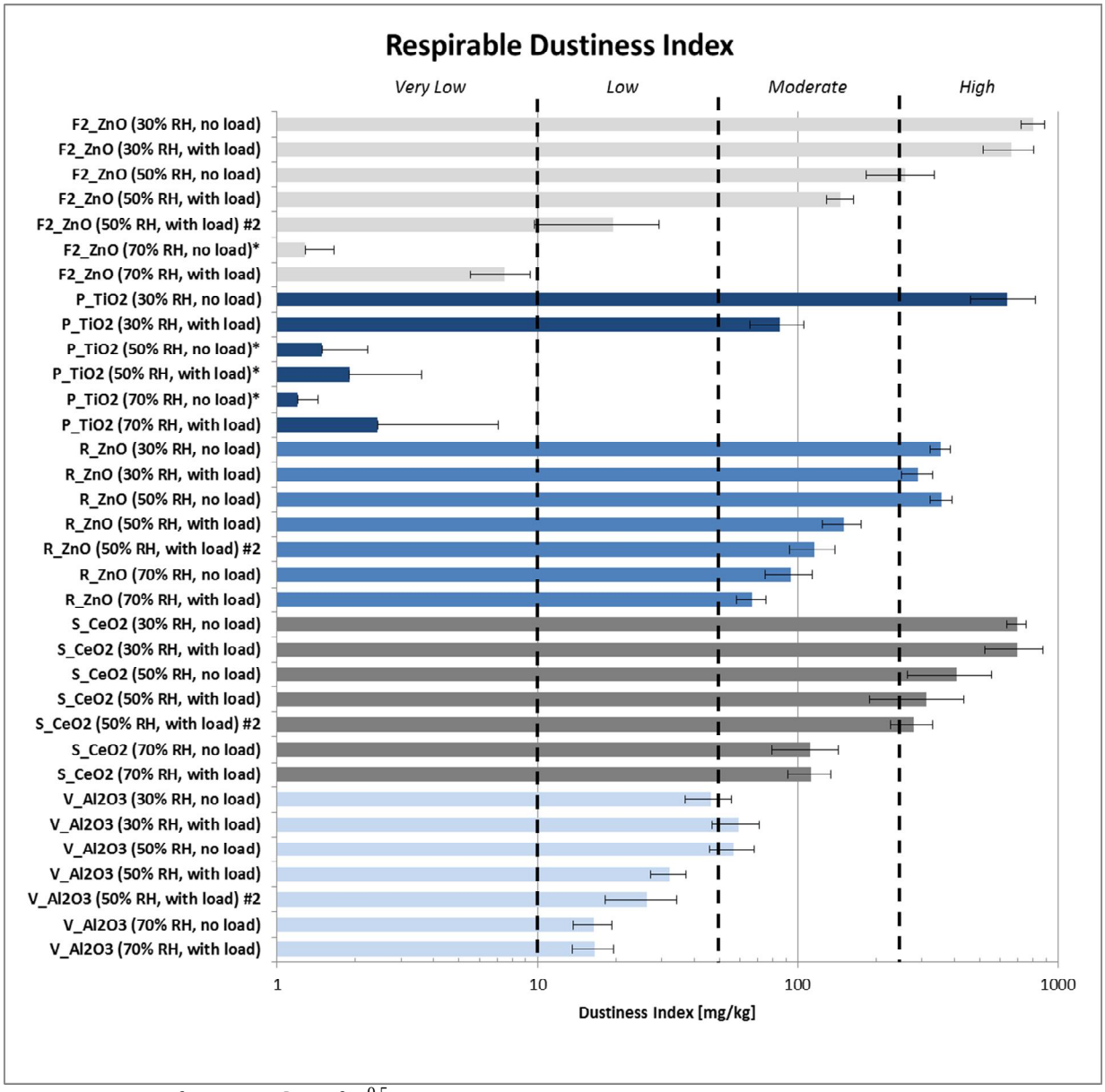

* Assuming a reference value of $\sigma^{0.5}$

Fig. 33 Graphical presentation of the respirable dustiness indices for all samples and conditions tested. The boundaries to the dustiness categories are indicated with the bold broken lines). Following the EN15051 convention for classification of powder dustiness denotes indices *Very Low* for <10 mg/kg, *Low* for between 10 and 50 mg/kg, *Moderate* between 50 and 250 mg/kg and *High* >250 mg/kg.

5.2) Particle Emission During Small Scale Manufacturing

Field measurements were conducted to assess NP emission during powder production, handling and packaging activities during small scale manufacturing. The principle of production was sol-gel synthesis. The activities with the highest potential of particle release or secondary particle formation were evaluated to be the process of high-temperature calcinations in an oven, as well as handling and packaging of the resulting powder inside a fume hood. Measurements covered production, handling and packaging activities of two NP powders, TiO_2 and ZnO. Particle measurements were carried out using high-resolution online particle monitors and sizers. Measurements were done both close to the activity (near-field) and in a background (far-field) position. A personal sampler for the worker was also used to measure respirable mass through gravimetrical analysis.

In all cases, an increased particle concentration was found in the air of the laboratory during the synthesis phases in the oven. However, the particle increase could not be clearly linked to emissions from the oven process. The size-distributions from the near field samples (manufacturing process) and the far field samples (background) were almost identical with a peak at ca. 80 nm. It was concluded that the events were linked to external particle sources, such as smoking, that occurred in neighbouring environments. The personal and stationary respirable dust exposure levels were below the detection limit, which was 0.10 mg.

As a conclusion, workplace measurements showed that there was no detectable process-related emission of NPs outside the fume-hoods in the sol-gel manufacturing at the small-scale laboratory. Weighing and packaging involving scooping of powder did not result in detectable emissions.

1.4 Please provide a description of the potential impact (including the socio-economic impact and the wider societal implications of the project so far) and the main dissemination activities and the exploitation of results.

The HINAMOX project has generated during the last three years a significant amount of basic research which brings a broader understanding of the complex interactions between nanoparticles, specifically of metal oxide NPs and biological matter both “in vitro” and “in vivo”.

This basic knowledge is fundamental to evaluate possible impact of NPs on human health and and have as well significant economical importance. The wide societal acceptance of the nanotechnology relies on that the consumers are sure that this technology will not bring harm to them or the environment. To ensure this a proper evaluation of the impact of different nanomaterials is compulsory. Metal oxide NPs, the focus of HINAMOX, are among the NPs with major applications nowadays being part of several products concerning household, beauty industry, electronics, soil remediation, fuels, etc that justify their importance regarding toxicological evaluation as well as being the focus of this project.

The problem of evaluating the impact of NPs is complex and requires multiple expertise and technical input as it has been shown in the technical memory. The wide scientific expertise gathered in HINAMOX was fundamental to achieve the complex goals of the project and to generate the unique and fundamental knowledge that the project generated.

One of HINAMOX most relevant technical development is the quantification “in vitro” and “in vivo” of NPs at cellular and organ level. In order to achieve that a complex work entailing the synthesis of NPs that can be traced i.e. fluorescent or radiolabelled, the application of advanced detection techniques such Ion Beam Microscopy or Positron Emission Tomography. This quantification can provide a major issue in regulatory testing since there could be a significant differences between applied doses of NPs and toxicologically relevant genuine doses actually observed in cells, organs and, finally, the whole organism, because the uptake of nanomaterials depends on physico-chemical, surface properties/modifications of the materials and the way of administration. The Genuine Dose is the central link between exposure and toxicity and can be considered as a key toxicological endpoint. Therefore, the quantification of the Genuine Dose can be the basis for systematic and comparable intracellular dose dependent toxicity studies between *in vitro* and *in vivo* tests. This can be fundamental on the design of “in vitro” relievable tests for the toxicological impact of NPs that can be “in vivo” validated. Knowing the Genuine Doses both “in vitro” and “in vivo” makes them comparable as well as their end points. In the same way, the Genuine Dose can be fundamental for the risk analysis of possible impact of NPs, becoming a crucial toxicological end point in itself.

The knowledge generated in HINAMOX on the impact of metal oxide NPs on human health with a strong focus on material science, in relating NP properties and characteristics with their toxicological end points can be applied as well in further developments of nanomaterials and complex mixtures entailing these nanomaterials that have industrial application, in order to improve materials properties with the scope of reducing their possible toxicity or reducing their potential risk of impact, what is called “safe by design”. This has in itself an important economical meaning and in long terms may be crucial for the industrial development associated with nanotechnology and other emerging technologies that may require improving their products to achieve their societal acceptance.

Scientific development and fundamental knowledge generation has been the central issue of the HINAMOX project. This basic knowledge is however fundamental for further developments in regulatory issues of nanomaterials and in the design of improved manufacture products. Therefore, HINAMOX impact is very wide. Scientifically HINAMOX lead to the generation of novel NPs with tailored properties, new routes of radio labelling were developed, Ion Beam Techniques have been applied for NP quantification and intracellular fate as well as Positron Emission Tomography for in vivo studies, among other achievements.

The society will benefit from HINAMOX results through the impact of the project in the regulation and possible application of the knowledge generated in the development of new products, having a positive impact on the industry in this particular issue as well.

The HINAMOX project, being conscious of the need of transferring the knowledge generated in the project to the different statements of the society and of the importance that the society becomes more aware of the advantages and risks of nanotechnology, promoted a series of dissemination activities approaching different stakeholders during the whole duration of the project. These activities included oral and poster presentations in scientific congresses, seminars, the organization of scientific meetings together with other European Projects, the periodic release of a newsletter every six month, the writing of scientific publications, the launching and continuous update of a project webpage and an active participation in the Nanosafety Cluster, which gathers the different actuators in Nanosafety within Europe.

Type of activities	Beneficiary	Title	Date	Type of audience
Conferences	ULEI	Interaction of metal oxide NPs with primary lung cells under simulated breathing, Annual Meeting of the European Respiratory Society , Wien, Austria.	01-05/09/2012	Scientific community
Press releases	HINAMOX Consortium	HINAMOX 6th Newsletter: Health impact of metal oxide nanoparticles: main achievements at a glance.	September 2012	Scientific community
Conferences	UVigo	Value of research in nanotechnology. From idea to company NANOIMMUNOTECH. Nanovalor Forum. Santiago de Compostela, Spain.	12/07/2012	Industry
Conferences	UVigo	Research on Nanomedicine. Instituto de Medicina Molecular, University of Lisbon, Faculty of Medicine. Portugal.	10/07/2012	Scientific community
Conferences	UVigo	Nanoparticles may not be inert to the immune system. III Encontro do INCT de Nanobiotecnología. UFG, Goiania, Brasil.	27-29/06/2012	Scientific community
Web/sites applications	HINAMOX Consortium	Nanopaprika.eu - The international Nanoscience Community 2012 http://www.nanopaprika.eu/profiles/blog/list?tag=HINAMOX	20/06/2012	Scientific community
Web/sites applications	HINAMOX Consortium	"Summary of EHS studies on nanotechnology funded through Europe's 7th Framework Programme". FrogHeart. http://www.frogheart.ca/?tag=hinamox	19/06/2012	Policy makers

Presentations	UVigo	Functionalizated magnetic nanoparticles for biodetection, imaging and separation of Mytilus galloprovincialis larvae using nitzipper®technology. Industrial Technologies 2012. Aarhus, Denmark.	19-21/06/2012	Industry
Conferences	CIC biomaGUNE	Síntesis, caracterización y biodistribución de nanopartículas de óxidos metálicos mediante Tomografía por Emisión de Positrones, 32º Congreso de la Sociedad Española de Medicina Nuclear e Imagen Molecular (SEMNIM), Cádiz, Spain.	13-15/06/2012	Scientific community
Conferences	CIC biomaGUNE	Synthesis, characterization and biodistribution of metal oxide nanoparticles by means of Positron Emission Tomography (PET), 9th World Biomaterials Congress, Chengdu, China.	01-05/26/2012	Scientific community
Presentations	ZJU	Oral presentation of "Cellular internalization of metal oxide nanoparticles and their influences on cell functions". 9th World Biomaterials Congress, Chengdu, China.	01-05/26/2012	Scientific community
Conferences	ZJU	Designed Biomaterials for Tissue Regeneration and Cellular Uptake. International Forum of Biomedical Materials: Nanobiomaterials for Tissue Regeneration. Hangzhou, China.	29/05-01/06/2012	Scientific community
Web/sites applications	HINAMOX Consortium	"HINAMOX - Health Impact of Engineered Metal and Metal Oxide Nanoparticles: Response, Bioimaging and Distribution at Cellular and Body Level" Danish National Research Centre for the Working Environment. www.arbejdsmiljoforskning.dk/en/projekter/HINAMOX	25/05/2012	Policy makers
Workshops	HINAMOX Consortium	Assessment of the biodistribution pattern and inflammatory response after acute administration of metal oxide Nps using Positron Emission Tomography, Workshop in Safety Issues and Regulatory Challenges of Nanomaterials, San Sebastián, Spain.	03-04/05/2012	Scientific community
Workshops	HINAMOX Consortium	Nanostructures and Immune system. Workshop in Safety Issues and Regulatory Challenges of Nanomaterials, San Sebastián, Spain.	03-04/05/2012	Scientific community
Press releases	HINAMOX Consortium	HINAMOX 5th Newsletter: Metal oxide internalisation in lung cells and biodistribution studies in mice	Apr 2012	Scientific community

Workshops	HINAMOX Consortium	International Workshop Meeting of the Cost Action FA0904 (Valencia, Spain) "Development of new safe PNFP and Development of new strategies to identify any critical interaction of PNFP with food" http://www.costfa0904.eu/cnr-ictp/html/61/	08-09/03/2012	Scientific community
Conferences	HINAMOX Consortium	NanoSafety Cluster (Dublin, Ireland) http://www.nanosafetycluster.eu/working-groups/4-database-wg.html	01/03/2012	Scientific community
Workshops	HINAMOX Consortium	"Cytotoxicity and uptake of metal oxide nanoparticles in human lung cells", Workshop of slide-based cytometry, Leipzig, Germany	March 2012	Scientific community
Conferences	HINAMOX Consortium	4th NanoImpactNet Integrating Conference and 1st QNano Integrating Conference (Dublin, Ireland) http://www.nanoimpactnet.eu/ http://www.nanosafetycluster.eu/news/33/66/NanoImpactNet-QNano-conference-From-theory-to-practice---development-training-and-enabling-nanosafety-and-health-research.html	27/02-02/03/2012	Scientific community
Conferences	HINAMOX Consortium	V Conferencia Anual de las Plataformas Tecnológicas de Investigación Biomédica: Medicamentos Innovadores, Nanomedicina, Tecnología Sanitaria y Mercados Biotecnológicos Fomentando la *Open Innovation*	14-15/02/2012	Policy makers
Web/sites applications	HINAMOX Consortium	"Health Impact of Engineered Metal and Metal Oxide Nanoparticles" NANOTEXNOLOGY http://www.nanotexnology.com/index.php?option=com_content&view=article&id=210:moya&catid=43	2012	Scientific community
Web/sites applications	HINAMOX Consortium	ENPRA/JRC. http://www.enpra.eu/	2012	Policy makers
Presentations	ULEI	"Quantification and colocalization of ENM in cells" Invited presentation at the Department of Pharmaceutical Nanotechnology, University of Saarbrücken	Dec 2011	Scientific community
Workshops	ULEI	"Cytotoxicity and uptake of metal oxide nanoparticles at A549 cells", Leipzig Life Sciences Research Festival,	Dec 2011	Scientific community

Workshops	ULEI	Study of nanoparticle uptake and quantification in lung cells by ion beam microscopy, Leipzig Life Sciences Research Festival	Dec 2011	Scientific community
Conferences	HINAMOX Consortium	International Conference on Safe Production and Use of Nanomaterials Nanosafe (NanoSafe 2010. Grenoble, France)	16-18/11/2011	Scientific community
Conferences	ULEI	"Interaction of metal oxide NPs with primary lung cells under simulated breathing", Annual Meeting of the German Society of Pneumology, Berlin	01/11/2011	Scientific community
Workshops	CIC biomaGUNE	A New Strategy to Label Metal Oxide Nanoparticles: Application to PK studies.	Novemb 2011	Scientific community
Conferences	ULEI	Interaction of metal oxide NPs with primary lung cells under simulated breathing, Annual Meeting of the European Respiratory Society , Wien, Austria	Novemb 2011	Scientific community
Workshops	UVigo	Invited Oral presentation: Methods to check biocompatibility , toxicity and immunogenicity (Braga, Portugal)	20/10/2011	Scientific community
Workshops	CIC biomaGUNE	Invited Oral presentation: "Nanotoxicology II: Challenges and opportunities in nanotoxicology" at the Nanotechnology and Nanomedicine course (Braga, Portugal)	20/10/2011	Scientific community
Workshops	UVigo CIC biomaGUNE	Nanotechnology and Nanomedicine Course at the Universidade de Braga (Braga, Portugal)	17-21/10/2011	Scientific community
Conferences	CIC biomaGUNE	Poster: Investigation of nanoparticle-cell interactions by fluorescence correlation specteoscopy, Nanosmat, Krakovia, Poland	17-21/10/2011	Scientific community
Conferences	CIC biomaGUNE	Oral presentation: Uptake, biological fate, biodistribution and toxicological studies of metal oxide nanoparticlesNanosmat, Krakovia, Poland	17-21/10/2011	Scientific community
Press releases	HINAMOX Consortium	HINAMOX 4th Newsletter: Looking at nanoparticles inside the cell	Octob 2011	Scientific community
Workshops	UVigo	ESCCA 2011 Conference (Dublin, Ireland) http://www.escca.eu/Meetings-Euroconferences/239/2011_Dublin/	13-17/09/2011	Scientific community

Conferences	UVigo	Human Nanotoxicology Meeting: "Cytotoxicity and immunogenicity of nanomaterials: studies at cellular and molecular level" (at the Chartered Institute of Environmental Health)	22-23/09/2011	Scientific community
Conferences	CIC biomaGUNE	EU Nanosafety Cluster: Linking Environment-Related Projects London, UK	22/09/2011	Scientific community
Conferences	ZJU	The 3rd Asian biomaterials congress	17/09/2011	Scientific community
Conferences	UVigo	Nanotechnology: Understanding cell biology (at the European Society for Clinical Cell Analysis. Dublin, Ireland)	14-17/09/2011	Scientific community
Conferences	ULEI	Invited Talk in frame cooperation: Nanomaterial-surfactant interaction (Halle, Germany)	15/09/2011	Scientific community
Conferences	UVigo	Regulatory testing of nanomaterials (at the Symposium NanoLCA. Barcelona, Spain)	08/09/2011	Scientific community
Press releases	UVigo	HINAMOX 3rd Newsletter: Response, Bioimaging and Distribution at Cellular and Body Level	Septemb 2011	Scientific community
Web/sites applications	HINAMOX Consortium	"HINAMOX (Health impact of engineered metal and metal oxide nanoparticles: Response, bioimaging and distribution at cellular and body level)" CORDIS http://cordis.europa.eu/search/index.cfm?fuseaction=result.document&RS_LANG&RS_RCN=12280417&q=	02/08/2011	Policy makers
Conferences	CIC biomaGUNE	Oral presentation: "Uptake, biological fate, biodistribution and toxicological studies of metal oxide nanoparticles" at NN11 conference at Tesaloniki, Greece	15/07/2011	Scientific community
Conferences	CIC biomaGUNE	Oral presentation on the HINAMOX project at Section on European projects on Nanomedicine at NN11 conference at Tesaloniki, Greece	15/07/2011	Scientific community
Conferences	CIC biomaGUNE	Oral presentation on general issues of Nanosafety at a round table on nanomedicine NN11 conference at Tesaloniki, Greece	14/07/2011	Scientific community
Presentations	ULEI	"Quantification and colocalization of ENM in cells" Presentation of the project HINAMOX at Yerevan State University	01/07/2011	Scientific community
Conferences	CIC biomaGUNE	Invited talk: Nanomedicine and nanotoxicity 2º Encontro do Instituto Nacional de Ciência e Tecnologia (INCT) em Nanobiotecnologia. Rio Grande, Acre, Brasil	27-29/06/2011	Scientific community

Conferences	ULEI	Trends in Colloid & Interface Science (at the Max Planck Institute of Colloids and Interfaces. Golm, Potsdam, Germany)	22-23/06/2011	Scientific community
Conferences	UVigo	Efectos en viabilidad celular debidos a Nps óxido metálicas (at the Congreso Nacional of the Sociedad Española de Inmunología. Pamplona, Spain)	08-11/06/2011	Scientific community
Workshops	CIC biomaGUNE	Oral presentation on promises of materials at the Nanosafety Cluster meeting at the Euronanoforum (Budapest, Hungary)	30/05-01/06/2011	Scientific community
Conferences	UVigo	Efectos en viabilidad y migración celular debidos a Nps óxido metálicas (at the IV Jornada de Investigación Biomédica. Vigo, Spain)	24/05/2011	Scientific community
Conferences	FIOH	Genotoxicity of Nanomaterials - Issues to Consider (at the Symposium: Safety issues of Nanomaterials along their life cycle. Barcelona, Spain)	04-05/05/2011	Scientific community
Conferences	ULEI	Poster: Quantification of nanoparticles uptake, their localization and toxicity at the single cell level (at Symposium NanoLCA: Safety issues of Nanomaterials along their Life Cycle. Barcelona, Spain)	04-05/05/2011	Scientific community
Conferences	CIC biomaGUNE	Synthesis of Radiolabelled NPs for biodistribution studies in animal models (at Symposium NanoLCA: Safety issues of Nanomaterials along their Life Cycle. Barcelona, Spain)	04-05/05/2011	Scientific community
Conferences	CIC biomaGUNE	Poster: Study of Cellular uptake and localization of cerium oxide nanoparticles at Symposium NanoLCA: Safety issues of Nanomaterials along their Life Cycle (Barcelona, Spain)	04-05/05/2011	Scientific community
Web/sites applications	HINAMOX Consortium	Symposium: Safety issues of nanomaterials along their life cycle" NANOfutures www.nanofutures.info/event/symposium-safety-issues-nanomaterials-along-their-life-cycle	04/05/2011	Policy makers
Articles published in popular press	HINAMOX Consortium	"Tan pequeñas como potentes" La Voz de Galicia (http://www.lavozdegalicia.es/vigo/2011/05/01/0003_201105V1C7992.htm)	01/05/2011	Civil society
Web/sites applications	HINAMOX Consortium	"Bilbao workshop looks at metal and metal oxide nanoparticle safety" NANOCODE http://www.nanocode.eu/content/view/202/40/	01/04/2011	Policy makers

Conferences	UVigo	Nanotecnologia y Sistema Inmune (at the Fundación Esteve (Barcelona, Spain)	29/04/2011	Scientific community
Workshops	CIC biomaGUNE	Organization of the workshop Nanosafety Nanotoxicology at the Industrial Forum of Imaginenano (Bilbao, Spain)	13/04/2011	Industry
Workshops	CIC biomaGUNE	Presentation of the project HINAMOX, Industrial Forum, Imaginenano (Bilbao, Spain)	11-14/04/2011	Industry
Workshops	FIOH	"Good Practices at working environment." at Nanosafety Nanotoxicology seminar Industrial Forum, Imaginenano (Bilbao, Spain)	11-14/04/2011	Scientific community
Workshops	UVigo	"Nanotoxicology."at Nanosafety Nanotoxicology seminar Industrial Forum, Imaginenano (Bilbao, Spain)	11-14/04/2011	Scientific community
Conferences	CIC biomaGUNE	Organization of a section on Nanotoxicology at the Imaginenano conference (Bilbao, Spain)	11-14/04/2011	Scientific community
Conferences	CIC biomaGUNE	"Synthesis of positron emitter labelled metal oxide nanoparticles for biodistribution studies by direct activation with high energy protons" at Imaginenano (Bilbao, Spain)	11-14/04/2011	Scientific community
Conferences	ULEI	"Quantification of Nanoparticle Uptake and their Colocalization with cell constituents at single cell level" at Imaginenano (Bilbao, Spain)	11-14/04/2011	Scientific community
Conferences	CIC biomaGUNE	Poster: "Cell uptake and cytotoxicity studies of metal oxide nanoparticles" INRS Occupational Health Research Conference 2011: Risks associated to Nanoparticles and Nanomaterials.	05-07/04/2011	Scientific community
Conferences	ULEI	Interaction of metal oxide NPs with primary lung cells under simulated breathing, Annual Meeting of the German Society of Pneumology (Dresden, Germany)	01/04/2011	Scientific community
Presentations	ULEI	"In vitro quantificatio of NM at sigle cell level" Invited presentation at the Federal Institute of Risk Assessment (Berlin, Germany)	01/04/2011	Policy makers
Web/sites applications	HINAMOX Consortium	"Imaginenano: Bringing together Nanoscience & Nanotechnology" http://www.imaginenano.com/INDUSTRY/Industry_Imaginenano.php?p=IS	01/04/2011	Policy makers

Press releases	UVigo	HINAMOX 2nd Newsletter: Uptake and Cytotoxicity effects of oxido-metallic nanoparticles	Apr 2011	Scientific community
Web/sites applications	ULEI	"Nanoparticle uptake, colocalization and toxicity at cellular level" ebookbrowse. http://ebookbrowse.com/ulei-HINAMOX-6-news-file-pdf-d87142610	24/03/2011	Scientific community
Conferences	UVigo	Nanoparticles and Antibodies: a Complex Alliance (at the BIT's 3rd Annual International Congress of Antibodies. Beijing, China)	23-25/03/2011	Scientific community
Conferences	ULEI and CIC biomaGUNE	3rd NanoImpactNet conference-Nanocluster (Lausanne, Switzerland)	17/02/2011	Scientific community
Press releases	HINAMOX Consortium	"Compendium of Projects in the European NanoSafety Cluster" (ftp://ftp.cordis.europa.eu/pub/.../compendium-nanosafety-cluster2010_en.pdf)	March 2010	Policy makers
Publications	UVigo	HINAMOX 1st Newsletter: Health impact of engineered metal and metal oxide nanoparticles	Octob 2010	Scientific community
Web/sites applications	CIC biomaGUNE	"HINAMOX" FoodDrink Europe: NanoTechnology- http://www.fooddrinkeurope.eu/industry-in-focus/topic/nanotechnology/eu-projects/	17/11/2009	Policy makers
Web/sites applications	HINAMOX Consortium	"European HINAMOX project analyses health impact of nanoparticles" nanowerk. http://www.nanowerk.com/news/newsid=13205.php	26/10/2009	Scientific community
Press releases	CIC biomaGUNE	"CIC biomaGUNE analiza el impacto en salud de nanopartículas presentes en las cremas solares" (http://www.basqueresearch.com/berria_irakurri.asp?Berri_Kod=2420&hizk=G#.UDT8e6niYvk)	26/10/2009	Civil society
Press releases	CIC biomaGUNE	"Analizan el impacto en salud de nanopartículas presentes en las cremas solares" (http://www.medifarmacia.com/Noticia.aspx?qs=ZHdmudCUjt9vVdrMeMtpsIp6p6AWbirc8Iend%2fPP9icri9%2bCVJMkJrRPXHNZczLj0avXf43mjPYBBbOBzhPTC0%2bcMqL9mtb)	23/10/2009	Industry

Press releases	HINAMOX Consortium	“European Project evaluates possible health impact of metal oxide nanoparticles” Bio Topics	23/10/2009	Industry
Articles published in popular press	HINAMOX Consortium	"Cremas solares: Se investiga si llevan nanopartículas tóxicas" El diario montañés (http://www.eldiariomontanes.es/20091022/sociedad/otras-noticias/investiga-llevan-nanoparticulas-toxicas-20091022.html)	22/10/2009	Civil society
Articles published in popular press	HINAMOX Consortium	“Investigan si las nanopartículas de las cremas solares son nocivas para la salud” La Vanguardia (http://www.lavanguardia.mobi/mobi/noticia/53809083053/Investigan-si-las-nanoparticulas-de-las-cremas-solares-son-nocivas-para-la-salud.html)	22/10/2009	Civil society
Articles published in popular press	HINAMOX Consortium	“Investigan si las nanopartículas de las cremas solares son nocivas para la salud” La Vanguardia (http://www.lavanguardia.mobi/mobi/noticia/53809083053/Investigan-si-las-nanoparticulas-de-las-cremas-solares-son-nocivas-para-la-salud.html)	22/10/2009	Civil society
Press releases	HINAMOX Consortium	“Investigan si nanopartículas de las cremas solares son nocivas para la salud” ADN.es (http://www.adn.es/tecnologia/20091021/NWS-1964-Investigan-nanoparticulas-nocivas-solares-cremas.html)	22/10/2009	Civil society
Articles published in popular press	HINAMOX Consortium	“Investigan si hay nanopartículas nocivas en cremas solares” DEIA, Bilbao, Spain. 22/10/2009 (graphic edition)	22/10/2009	Civil society
Press releases	CIC biomaGUNE	“CIC biomaGUNE analiza el impacto en la salud de nanopartículas presentes en las cremas solares”. Published in the web www.noticiasmedicas.es	22/10/2009	Civil society
Articles published in popular press	CIC biomaGUNE	“CIC biomaGUNE lidera un proyecto europeo que analizará la toxicidad de nanopartículas de óxidos metálicos”. Article published in “Basque News”. (http://www.euskadi2015.net/FOROCOMPETITIVIDAD/cs/tabid/843/articleType/ArticleView/articleId/1829/CIC-biomaGUNE-lidera-un-proyecto-europeo-que-analizara-la-toxicidad-de-nanoparticulas-de-oxidos-metalicos.aspx)	22/10/2009	Civil society

Articles published in popular press	HINAMOX Consortium	"Investigan si nanopartículas " published in ABC web edition (http://www.abc.es/Agencias/noticia.asp?noticia=147997)	21/10/2009	Civil society
Articles published in popular press	HINAMOX Consortium	"Las cremas solares a examen". El Diario Vasco, España (http://www.diariovasco.com/20091021/mas-actualidad/sociedad/cremas-solares-san-sebastian-investigacion-200910211821.html)	21/10/2009	Civil society
Press releases	HINAMOX Consortium	"CIC biomaGUNE lidera un proyecto sobre toxicidad de nanopartículas" Euskadi+innova (http://www.euskadinnova.net/es/innovacion-tecnologica/noticias/biomagune-lidera-proyecto-investigacion-sobre-toxicidad-nanoparticulas/5894.aspx)	17/10/2009	Civil society
Articles published in popular press	HINAMOX Consortium	"CIC biomaGUNE to lead European project HINAMOX" (http://www.eitb.com/en/news/detail/261428/cic-biomagune-lead-european-project-hinamox/)	07/10/2009	Medias
Press releases	HINAMOX Consortium	"European project evaluates possible health impact of metal oxide nanoparticles" Nanowerk. (http://www.nanowerk.com/news/newsid=12904.php)	05/10/2009	Policy makers
Press releases	HINAMOX Consortium	"Análisis de toxicidad de nanopartículas de óxidos metálicos" Boletín de Vigilancia Tecnológica, Spanish Ministry of Defence	02/10/2009	Policy makers
Web/sites applications	HINAMOX Consortium	"Health impact of engineered metal and metal oxide nanoparticles: Response, bioimaging and distribution at cellular and body level" istworld http://www.ist-world.org/ProjectDetails.aspx?ProjectId=7f840076a5944153ada998be575067a6&SourceDatabaseId=018774364ea94468b3f4dec24aa1ee53	01/10/2009	Policy makers
Press releases	HINAMOX Consortium	"Health Impact of Engineered Metal and Metal Oxide Nanoparticles", Azonanotechnology (http://www.azonano.com/newsarchive.asp?startdate=20091001&enddate=20091031)	31/09/2009	Scientific community
Press releases	HINAMOX Consortium	"Scientists Examine Health Impact of Engineered Metal Nanoparticles Present in Sunscreen" (http://www.nano.org.uk/news/203/)	27/09/2009	Civil society

Press releases	HINAMOX Consortium	"CIC biomaGUNE is to lead an European project that will test the toxicity of the nanoparticles in metal oxides" (http://www.cicbiomagune.es/secciones/noticias/noticias_detalle.php?idioma=en&id_noticia=33)	18/09/2009	Scientific community
Web/sites applications	HINAMOX Consortium	www.hinamox.eu	01/09/2009	Scientific community
Press releases	CIC biomaGUNE	"CIC biomaGUNE to lead European project HINAMOX ". (http://www.eitb.com/news/technology/detail/261428/cic-biomagune-to-lead-european-project-HINAMOX/)	10/07/2009	Civil society
Web/sites applications	CIC biomaGUNE	"HINAMOX" Nanosafety cluster www.nanosafetycluster.eu/home/eu-nanosafety-cluster-projects/seventh-framework-programme-projects/HINAMOX.htm	01/07/2009	Policy makers

The project organised the following two meetings: Nanosafety Issues of Nanomaterials Along Their Life Cycle (NANOLCA), organised together with the European Projects NEHP and NANOPOLYTOX in Barcelona, 2-3 May 2011; and NANOLCA II organised with the above mentioned projects , the EU project EMPRA and the Joint Research Centre of the European Commission in San Sebastian, 3-4 May 2012.

Both meetings were attended by a wide audience with the participation of scientific regulators, representatives of regional, national and European institutions.

The main focus of the meetings was to analyse the importance of life cycle analysis in the study of the behaviour and fate of nanomaterial based products and its consequence in the risk assessment of these products. Additionally, other scientific topics related to materials, toxicology, general risk assessment and ecotoxicity were considered. During the meeting the advances and achievements of the organising projects were presented to the audience.

Title	Tracing nanoparticles in vivo: a new general synthesis of positron emitting metal oxide nanoparticles by proton beam activation	Assessment of the evolution of cancer treatment therapies	Nanoparticle uptake and their co-localization with cell compartments - a confocal Raman microscopy study at single cell level	Cytotoxicity effects of oxido-metallic nanoparticles in tumor cell lines
Main Author	Jordi Llop	Manuel Arruebo, Nuria Vilaboa, Berta Sáez-Gutierrez, Julio Lambea, Alejandro Tres, Mónica Valladares and África González-Fernández	I Estrela-Lopis, G Romero, E Rojas, S E Moya and E Donath	T Lozano, M Rey, E Rojas, S Moya, J Fleddermann, I Estrela-Lopis, E Donath, B Wang, Z Mao, C Gao, A Antipov, A. González-Fernández

Title of the periodical or the series	Chemistry World	Cancers	Journal of Physics: Conference Series	Journal of Physics: Conference Series
Number, date or frequency	Volume 137, Fortnightly	Volume 3, Issue 3. Quarterly	Volume 304 Number 1. Quarterly	Volume 304 Number 1. Quarterly
Publisher	Royal Society of Chemistry	MDPI Publishing	IOP Publishing	IOP Publishing
Place of publication	Cambridge, UK	Basel, Switzerland	London, UK	London, UK
Date of publication	September 20, 2012	August 12, 2011	July 6, 2011	July 6, 2011
Relevant pages		3279-3330	12017	12046
Permanent identifiers (if available)	IF: 4,23		IF: 3,849	IF: 3,849
Open access is/will be provided to this publication	Yes	Yes	Yes	Yes

1.5 Please provide the public website address (if applicable), as well as relevant contact details.

www.hinamox.eu